Numerical and experimental optimization analysis of a jaw crusher and a bubble column reactor

Daniel Legendre

Doctor of Technology Thesis

Thermal and Flow Engineering Laboratory

Faculty of Science and Engineering

Åbo Akademi University

Turku, Finland 2019

Numerical and experimental optimization analysis of a jaw crusher and a bubble column reactor

Daniel Legendre

Doctor of Technology Thesis

Thermal and Flow Engineering Laboratory

Faculty of Science and Engineering

Åbo Akademi University

Turku, Finland 2019

Supervision
Professor Ron Zevenhoven
Professor Henrik Saxén
Thermal and Flow Engineering Laboratory
Åbo Akademi University
Turku, Finland.

Opponent and reviewer
Professor Ville Alopaeus
Chemical and Metallurgical Engineering
Aalto University
Espoo, Finland.

Reviewer
Docent, Dr. Cataldo De Blasio
Energy Technology
Åbo Akademi University
Vaasa, Finland.

ISBN 978-952-12-3822-2
ISBN 978-952-12-3823-9 (pdf)
Painosalama Oy
Turku, Finland 2019

Preface

The research work presented in this thesis was made possible and supervised by prof. Ron Zevenhoven and prof. Henrik Saxén who are acknowledged for many years of research funding, assistance during the experimental work and help with getting the research papers published. It was conducted in collaboration of Aalto University in Espoo, Finland (prof. Mika Järvinen) and Chalmers University of Technology in Gothenburg, Sweden (prof. Srdjan Sasic).

Financial support was received from the KH Renlund Foundation, the Doctoral Program in Energy Efficiency and Systems (GSEES), the CLIC Oy Carbon Capture and Storage Program (CCSP) Graduate School in Chemical Engineering (GSCE), Tekes/Aalto University TUTL project X2PCC, Stiftelsen Åbo Akademis Jubileusfond 1968, a three-month grant by the Dean of the faculty and a scholarship of Åbo Akademi's Rektor. All these persons and institutions are gratefully acknowledged.

Thanks go to Martin Slotte for donating 40% of his GSEES scholarship, Hannu-Petteri Mattila for taking care of the CLIC Oy CCSP project reporting and to Alf Hermanson, Vivéca Sundberg and the rest of the team at Thermal and flow engineering laboratory at Åbo Akademi.

Dedicated to my family. And I will forever be grateful to my brother Cesar for being my helping hand even in the most difficult times.

Abstract

More and more awareness is now raising in terms of sustainability of industrial processes. Thus the necessity to improve energy efficiency of diverse devices or simplify process schemes arises. Therefore, the importance of increasing the efficiency of these processes energy and material usage as means to reduce harmful emissions has increased. The present research involves the numerical modelling and further experimental analysis of two different process equipment: crushing and grinding (comminution) of ore materials and bubble swarm dissolution in a reactor. Numerical methods are expanded as means to obtain a physical description relevant for engineering purposes. Moreover, experimental methods are developed to sustain validity of the simplifications imposed on the numerical analysis. Concisely in the comminution case, a primary crusher machinery widely employed in industry known as a jaw crusher is used as center for optimization and modelling efforts. This is performed with the goal to explain and describe how energy is used during the crushing and grinding process and how it can be improved. It is widely acknowledged that crushing and grinding machinery are highly inefficient if the study is based only on energy requirements. Typically, estimated values $<10\%$, with most energy dissipated as heat, deformation, noise and internal crack propagation in the ore. First, an energy efficiency is defined in terms of machinery energy use and after-crushed particle size; with the idea to link new surface area created by material breakage to the amount of energy required to produce an effective particle segmentation. Second, a study on design methods for jaw crusher design through empirical methods, allows to estimate rough machinery dimensions and operating conditions for different selection criteria. However, these methods do not provide an insight into the actual particle breakage phenom-

ena. Further on, the development of a Discrete Element Method (DEM) model, widely used for the description of granular materials, allows to generate a dynamic model capable to mimic jaw crusher operating conditions. Despite of high computational requirements this gives results comparable to industrial applications in the field of crushers. The current research is based on the fundamentals that allow to reproduce breakage patterns on simulated particle agglomerates. To complement DEM models, an experimental strategy was designed and tested allowing to compare energy usage of a laboratory scale jaw crusher with new area created of crushed $\cong 600$ gr pieces of limestone rock. This method in principle can be applied to any type of comminution machinery regardless its size and could be linked to simulations efforts.

As a second case, the importance of bubble swarm dissolution arises with the intention of simplify downstream flow conditions of the so-called Slag2PCC process for mineral carbonation. This is one example of many carbon capture and utilization (CCU) processes being developed worldwide. As a carbonation reactor without any exhaust gasses, i.e. 100% CO_2 dissolution would imply simplifications on extra equipment for gases re-circulation in the reactor. In the first place, the study is focused on the smallest yet relevant phenomena of the reactor; a single dissolving bubble on water to further expand the analysis towards reactor operating conditions. As part of this research a hybrid CFD – Lagrangian bubble tracking method was developed to obtain preliminary results on bubble dissolution orders of magnitude and reactor design dimensions. Consequently, an experimental facility was built. With the use of a high-speed camera, free rising CO_2 bubbles were tracked in a 2 m height bubble tower. Not only the diameter reduction of the bubbles is evidenced but also their continuous shape transition from wobbly bubbles towards a more spherical bubble flow as the initially 5 mm bubbles dissolve. Results proved to be comparable to previous estimations on very disperse bubbly flows. Subsequently, a modification to the experimental facility with the inclusion of pitched blade impellers was made to measure CO_2 bubble flow on actual operating conditions of a reactor. The evolution of CO_2 bubble size distributions in terms of vertical displacement was measured and a positive influence of the mixing intensity on the bubbly flow dissolution was shown. Results presented could aid the development of multiphase flow models at higher gas volume fractions.

Svensk sammanfattning

Allt mer uppmärksamhet fästs idag vid hållbarheten hos industriell produktion och därför har vikten av att minska skadliga utsläpp och att effektivera processernas energi- och materialeffektivitet ökat. Ett användbart redskap i sådan processutveckling är modeller som avbildar verkligheten i liten skala eller numeriskt genom simulering. I föreliggande arbete studerades två viktiga industriella delprocesser: krossning och malning av malm, samt gasupplösning från bubbelsvärmar i vätskor. För ändamålet utvecklades numeriska och fysikaliska modeller, där de senare bl.a. utnyttjades för att verifiera de förenklingar som gjordes i de förra.

Det är ett välkänt faktum att krossnings- och malningsprocesser uppvisar mycket liten verkningsgrad i avseende på tillgodogjord energi. I regel utnyttjas mindre än 10% , av energin för krossningen/malningen medan den största delen ger upphov till friktionsvärme, deformering, (o)ljud och intern sprickpropagering i partiklarna. I avhandlingen studerades en primärkross, en s.k. käkkross (eng. jaw crusher), som allmänt används i industrin. Krossen modellerades matematiskt för att uttrycka energibehovet och därefter för optimering av krossningsprocessen med avsikten att minimera energiåtgången. Först utvecklades ett uttryck för att beskriva energieffektiviteten som funktion av maskinens energibehov och kornstorleken efter krossningen på basis av idén att koppla partikelyta som uppstått genom brott till energiåtgången för att producera en effektiv partikelsegmentering. Därefter utfördes en studie av empiriska designmetoder för käkkrossar, vilket gjorde det möjligt att grovt estimera maskindimensioner och driftbetingelser för olika krossningsbetingelser. Dessa metoder kan emellertid inte ge insikter i hur partiklarna krossas och nedbryts. Idag kan dock

sådana fenomen studeras med den s.k. diskreta elementmetoden (eng. Discrete Element Method, DEM) som används för att beskriva partikelflöden matematiskt. Denna numeriska metod gör det möjligt att skapa en dynamisk modell, som beskriver förloppen i en käkkross. Trots att de beräkningsdryga simuleringarna kräver förenklingar för att man skall kunna lösa problemet inom rimlig tid, visar resultaten god samstämmighet med vad som observeras i industriella krossar. Man kunde t.ex. reproducera brottsmönstren hos partikelagglomerat. För att komplettera DEM-modellen gjordes även experiment vilka möjliggjorde en jämförelse av energiåtgången i en käkkross i laboratorieskala. I experimentet studerades den nya ytan som skapades vid krossning av ca 600 grams kalkstensstycken. Den experimentella metoden kan i princip tillämpas på vilket typ av malningsförlopp som helst oberoende av storlek och resultaten kan jämföras med simulerade värden och kan användas för modellvalidering.

Det andra problemet som studerades i avhandlingen uppstått när man önskar förenkla ett delsteg i den s.k. Slag2PCC-processen där CO_2 fixeras genom karbonatisering. Denna process är ett av flera alternativ för koldioxidavskiljning och –användning (eng. Carbon Capture and Utilisation, CCU), som idag studeras aktivt för att minska koldioxidutsläpp och klimatändring. I delsteget där (avskilda) koldioxidbubblor upplöses i en lösning, för att senare bindas till mineralen, studerades svärmar av stigande bubblor i en vattenlösning. Om alla CO_2–bubblor kunde upplösas fullständigt har man en karbonatiseringsreaktor utan gasutsläpp, vilket avsevärt skulle förenkla processteget då man inte behöver utrustning för återförande av gaserna. Först studerades ett förenklat men ändå relevant delproblem i reaktorn, dvs beteendet hos enstaka bubblor, varefter analysen utvidgades till att beakta förhållandena i hela reaktorn. Som en del av denna forskning utvecklades en CFD–Lagrange-hybridmetod för att kunna simulera bubblornas rörelse och förhållandena vid dessa, vilket gav estimat av bubblornas upplösningshastighet samt lämplig reaktordesign. På basis av detta byggdes en pilotmodell i laboratorieskala. Med hjälp av en höghastighetskamera kunde fritt stigande CO_2-bubblor följas över en höjd av 2 m i den vertikala transparenta reaktorn. Med hjälp av resultaten från videosekvenserna kunde inte endast bubblornas krympning studeras utan även deras kontinuerliga formändringar. De visade sig att de ursprungliga 5

mm:s svajande icke-sfäriska bubblorna högre upp i reaktorn bildade sfäriska mindre bubblor som snabbt upplöstes. Resultaten visade sig vara jämförbara med vad som tidigare konstaterats för dispergerade bubbelflöden. På basis av observationerna modifierades den experimentella anläggningen så att reaktorn försågs med propellrar för omrörning för att bättre beskriva förhållandena i verkliga reaktorer. Bubblestorleksfördelningens utveckling i vertikalled uppmättes och omrörningsintensiteten inverkan på bubbelupplösningshastigheten studerades. De resultat som erhölls kan även användas vid utvecklingen av matematiska modeller för gas-väska-multifassystem där gasandelen är hög.

List of publications

The publications presented at the end of this thesis will be referred using the Roman numerals as given in the following list:

I. D. Legendre and R. Zevenhoven, "Assessing the energy efficiency of a jaw crusher". Energy, vol. 74, pp. 119–130, 2014.

II. D. Legendre and R. Zevenhoven, "A numerical Euler – Lagrange method for bubble tower CO_2 dissolution modeling". Chem. Eng. Res. Des., vol. 111, pp. 49–62, 2016.

III. D. Legendre and R. Zevenhoven, "Detailed experimental study on the dissolution of CO_2 and air bubbles rising in water". Chem. Eng. Sci., vol. 158, pp. 552-560, 2017.

IV. R. Zevenhoven, D. Legendre, A. Said, and M. Järvinen, "Carbon dioxide dissolution and ammonia losses in bubble columns for precipated calcium carbonate (PCC) production". Energy, vol. 175, pp. 1121-1129, 2019.

V. D. Legendre and R. Zevenhoven, "Image analysis assesment of the effect on mixing on aqueous dissolution of CO_2 and air bubble swarms in a bubble column". Chem. Eng. Res. Des., vol. 146, pp. 379-390, 2019.

List of related publications

Besides the above contributions, the author of this thesis has participated in conferences and meetings with non-reviewed publications, reports and presentations, as listed below, on the field of modelling and experimental analysis :

VI D. Legendre, "Assessing the energy efficiency of jaw crushers". MSc. Thesis. Åbo Akademi. Turku, Finland, 2012.

VII. D. Legendre and R. Zevenhoven, "Assessing the energy efficiency of jaw crushers".in Proceedings of ECOS 2013 - the 26th International Conference on Efficiency, Cost, Optimization, Simulation and Environmental Impact of Energy Systems. Guilin, China, July 2013, paper A018.

VIII. D. Legendre and R. Zevenhoven, "A numerical Euler - Lagrange method for bubble tower CO_2 dissolution modeling". Comsol conference, October 2015. Grenoble, France.

Contributions of the author

The author of this thesis designed and performed most of the experimental and theoretical work presented in the thesis. The planning of the construction and design of the experiments were also performed by the author, with the valuable help of colleagues.

Publication I: The present author conducted and designed the laboratory experiments, developed the DEM simulations, analyzed the results and wrote the paper, under the supervision and with assistance of the co-author.

Publication II: The present author developed the models and performed the simulations presented in the publication, analyzed the results and wrote the paper, under the supervision and with assistance of the co-author.

Publication III: The present author designed and constructed the experimental facility of the paper, conducted the laboratory experiments and developed the image analysis algorithms. The author also analyzed the results and wrote the paper under the supervision and with assistance of the co-author.

Publication IV: The present author performed the experiments and developed the image analysis algorithms given in section 2 of the publication. The other parts of the manuscript were developed by the first author (Prof. Zevenhoven) in collaboration with the third and fourth co-authors (Prof. Järvinen and Dr. Said).

Publication V: The present author designed and constructed the mod-

ified experimental facility, conducted the laboratory experiments and developed the image analysis algorithms further. The author also analyzed the results and wrote the paper under supervision and with assistance of the co-author.

List of abbreviations and symbols

B&W	Black and white
CCU	Carbon capture and utilization
CFD	Computational fluid dynamics
DE	Differential evolution
DEM	Discrete element method
FEM	Finite element method
LES	Large eddy simulation
NBB	Number of broken bonds
PCC	Precipitate calcium carbonate
pdf	Probability density function
SGA	Simple genetic algorithm
Slag2PCC	Process concept for production of precipitated calcium carbonate from steel slags
URANS	Unsteady Reynolds averaged Navier-Stokes
ÅA	Åbo Akademi university

a	Ellipse fit minor semi-axis
$A_{created}$	New surface area created
A_{sup}	Bubble surface area
b	Ellipse fit mayor semi-axis
c	Shape parameter

C_A	Bubble wet interface concentration
C_{Bulk}	Bulk concentration of the surrounded liquid
C_K	Kick index for coarse crushing
$Cos(\theta)$	Motor power factor
CO_2	Carbon dioxide
C_R	Rittinger index for ultra fine grinding
D	Reactor diameter
d	Scale parameter
D_{Bubble}	Bubble diameter
D_{fsm}	Final surface mean diameter
$Diameter_{32}$	Sauter mean diameter
D_{ism}	Initial surface mean diameter
E	Young modulus
$E_{Equipment}$	Energy usage
$\overrightarrow{F}_{Bouyancy}$	Buoyancy force
$\overrightarrow{F}_{Drag}$	Drag force
$\overrightarrow{F}_{Gravity}$	Gravity force
$\overrightarrow{F}_{i}$	Force representing virtual mass term, fluid history effects, deformation effects and other forces acting on a bubble
$\overrightarrow{F}_{Lift}$	Lift force
F_r	Roughness factor correction ($1 \leq F_r \leq 3$)
$\mathcal{F}_{Weilbull}$	Weilbull probability density function
G	Jaw crusher gape
G_{Shear}	Shear modulus
H	Reactor height
I_{rms}	Root mean squared current intensity
k	Constant related to the strength of the rock
k_{mass}	Mass transfer coefficient
L_t	Jaw crusher throw
M	Mass of the crushed rock
m	Bubble mass
Min_{Per}	Minimum passing percentage feed to the crusher
n	Constant related to the strength of the rock
$P_{Comminution}$	Comminution power consumption
$P_{Crusher}$	Crusher power consumption related to shaft power
P_{Elec}	Tri-phase electrical motor power consumption
P_{Empty}	Power consumption of an empty crusher
$P_{Equipment}$	Equipment power consumption

Q_A	Mass rock flow
R	Jaw crusher reduction ratio
R_{Bond}	Radius of the bond
Re	Reynolds number
$R_{Particle}$	Particle radius
S	Surface area
t	Time
T_R	Rayleigh time
$\overrightarrow{V}_{Bubble}$	Bubble velocity
V_{rms}	Root mean squared voltage
w	Jaw crusher width
W_i	Bond index for crushing
x	Mute variable

γ	Material fracture surface energy
$\gamma_{Simulation}$	Simulation fracture surface energy
ΔS_{EN}	Specific surface energy
ΔS_{Power}	Specific surface energy per unit of mass
$\eta_{Electric}$	Electrical efficiency of tri-phase motor
$\eta_{EnergyTotal}$	Equipment total energy efficiency
η_{Limit}	Theoretical limit efficiency
$\eta_{PowerTotal}$	Total power consumption efficiency
ν	Poisson modulus
ρ	Density
σ_{max}	Maximum normal stress
τ_{max}	Maximum tangential shear stress
ϕ_A	Bubble mass time derivative
χ	Aspect ratio
Ω	Toggle speed

Contents

Chapter 1

Introduction

In today's engineering world, the necessity of a more optimal use of resources and energy is the driving force towards more versatile and accurate designs of diverse types of machinery. This is one of the efforts to reduce and mitigate the CO_2 emission to the atmosphere. Nevertheless, to reach such a specific goal through more efficient processes, first a clear understanding of the underlying physical phenomena must be described in useful terms for engineering applications. These fundamental physical descriptions can be mathematically rearranged with some simplifications, to further develop into models that in principle should be able to explain how the system behaves. Certainly, no model represents an absolute truth, thus certain limitations are imposed on its applicability. Therefore, experimental verification is required, either to corroborate the validity of the model developed, modify or just discard it.

The presented research thesis acts as a compendium of papers that aim to pursue a more accurate understanding of two distant physical phenomena such as: a) crushing and grinding of ore materials and b) CO_2 bubble swarm dissolution. Although both processes in principle are not related, the basic engineering approach on how to describe their internal fundamental laws and producing suitable models that aid towards an optimized outcome is identical. In the case of crushing and grinding, the desired outcome is to operate a jaw crusher in the most

energy efficient way. Furthermore, in the case of bubble swarm dissolution the goal is to establish the characteristics of a reactor capable to obtain a complete dissolution of CO_2 without any gas exhaust.

Even if these two problems are separate and may seem rather unrelated, both are present in process of re-using steel slag for the purpose of CO_2 mineralization. In the production of calcium ions necessary for the precipitation of calcium carbonate, the size distribution of the solid raw material (e.g., steel slag, limestone or any other alkaline Ca-rich industrial residue) plays a crucial role for the overall capacity of the mineralizing plant. Furthermore, literature reports that particle size distribution and reaction temperature are the most important factors affecting the quality of the mineralization process [1]. In the very same process, the dissolution of gaseous CO_2 into a liquid phase is also of central importance for an efficient precipitation of calcium carbonate [2].

One of the routes to mineral carbonation is the so-called Slag2PCC process, designed in cooperation between Aalto University and Åbo Akademi University in Finland. This is a continuous process for CO_2 capture and utilization that includes mixers, a bubble reactor, inclined settlers and filters for precipitated particles. Carbon dioxide is dispersed in an aqueous solution that contains dissolved calcium, producing precipitated calcium carbonate (PCC) particles. Since the solution used also contains dissolved ammonia with a certain vapor pressure, an exit stream of unreacted CO_2 would also contain ammonia. This would complicate the process by requiring an additional ammonia separation.

The two research topics of the present doctoral thesis are both related to the Slag2PCC process: The first one, i.e., efficient crushing and grinding of a bulk material (e.g., limestone, solid slag, etc.) is of importance for an efficient production of a solution rich in calcium ions necessary for the precipitation of calcium carbonate. The second topic is of central relevance for the carbonation process in a reactor where a stream of carbon dioxide bubbles is injected to be dissolved into the liquid phase.

In Paper I, the energy consumption is certainly one of the major concerns in crushing and grinding, i.e. comminution of rock, since com-

minution process has always been related with low energy efficiency. The goal of this work is to find ways to assess energy efficiency of size reduction processes. A jaw crusher is taken as a representative example. Mainly three strategies engaged the development of this paper: simple genetic algorithms, experiments and discrete element method simulations.

Paper II defines the fundamentals of bubble dissolution as a combination of force balances and the theory mass transfer for boundary layers. A one-way coupling simulation was developed for a dissolution reactor for CO_2 in water. The solution may contain dissolved calcium resulting in production of precipitate calcium carbonate (PCC). With its respective restrictions and approximations, rough bubble reactor dimensions were estimated to obtain a total bubble swarm dissolution at low gas volume fractions. The next step is presented in Paper III, where using the reactor dimension estimations from Paper II, a bubble tower of similar size is constructed. The goal is to corroborate the dissolution dynamics of single free raising bubble as a first experimental analysis. Using a high-speed camera and with the development of a single bubble tracking algorithm, the evolution of CO_2 bubble diameter are observed to decrease, quite well following previous numerical estimations.

Finally, the goal is to reach near-reality operating conditions of a bubble dissolution reactor as described in Paper IV and V. Design modifications to the bubble tower involved the inclusion of four pitched blade impellers with a variable speed motor. A qualitative estimation of bubble swarm dissolution indicates a slight positive influence of impeller rotational speed inducing faster dissolution in CO_2 bubbles. As described in Paper V, a quantitative method allows for measuring the effect of dissolution on CO_2 bubble swarm by estimating bubble size distributions as function of reactor height and impeller speed.

Chapter 2

Crushing and grinding

Crushing and grinding processes of ore materials (comminution) are designed to obtain a pre-determined particle size distribution rather than to have low power consumption. In a general, a comminution process has always been related with low efficiency rates. Nowadays, power consumption and therefore efficiency of practically any kind of equipment is becoming more important, as one effort to minimize CO_2 emissions globally [3]. Current research is more and more focused on the energy use in mining industry, showing that 40% of energy used in mining goes to overcome friction [4]. In principle, an optimized design of crushers may help reduce friction within the machinery, which could reduce power consumption in this area.

There exist several kinds of comminution equipment. With different manners of imparting forces on the ore, each of them is specifically designed for a certain reduction size and flow capacity. Gupta and Yan [5] list the most representative design models of comminution machinery in industry as:

- Jaw crusher.
- Ball mills.
- Tubular rod mills.

- Gyratory (cone) crusher.
- Vibration mills.
- Autogenous and semi-autogenous mills.
- Roll crusher.

2.1 Historical overview

It is well known that, in terms of energy usage in today's mining industry, comunition processes stand for a large section of all the energy consumption. One important research work addressing energy efficiency on comminution machinery was developed by Fuerstenau and Abouzeid [6]. This was centred on ball mills, where the efficiency was based on the specific energy needed to produce a given amount of new surface. This work was based on a single particle breakage and the energy needed to rotate the ball mill chamber.

Moreover, Schoenert [7] gave one of the first estimations on experimental single particle breakage for quartz rocks, with an energy requirement of 0.02 m^2/J. This gave the opportunity to Mortsell and Svensson [8] to make the first estimations of energy efficiency, obtaining that in a ball mill about 85% of the energy input is dissipated.

This is indeed a coherent manner to estimate an energy efficiency. However, a lot of uncertainties arise from the way of calculating the energy usage for a single particle breakage that are estimated from experimental data and diverse theoretical approximations.

Within these background works, the first research question of Paper I arises as:

- How to assess and quantify the energy efficiency of crushing and grinding process for industrial applications?

One of the first simulation attempts to model rock breakage was developed by Potyondy and Cundall [9]. They showed promising results on the breakage behaviour of a modelled block of granite by means of Discrete Element Method, using bonded particle rupture to mimic the breakage phenomena. Results were promising and agglomerate crack propagation behaviour showed realistic results comparable to actual real material behaviour. More concisely an application of this method to jaw crushers was made by Refahi et al. [10], where the clear applicability of DEM bonded models to jaw crushers was demonstrated, using FEM stress analysis. As a consequence the second research question of Paper I arises as:

- Can DEM simulations or empirical equation modelling aid on efficiency improvement and to reduce energy losses in comminution machinery?

2.2 A general efficiency definition

So far, there is not a solid definition of ”efficiency” in comminution processes, although it is understood that it is inefficient if the discussion is based exclusively on power requirements. Therefore, no reasonable assessment criteria exist of how much the performance of particle size reduction can be improved [11]. One of the main studies concerning energy distribution in crushers concluded the energy usage is divided as follows [12].

- In producing elastic deformation of the particles before fracture occurs.
- In producing inelastic deformation which results in size reduction.
- In causing elastic distortion of the equipment.
- In friction between particles and between particles and the machine.

- In noise, heat and vibration in the plant.

Typically less than 1/10 of the total input energy is utilized by the size reduction process itself [12]. The energy utilization of a general comminution process can be improved via two general approaches:

a) **Approach A:** increasing the amount of cracks in the material as a pre-treatment to obtain lower Bond index values (W_i) [13]. Thus, it is necessary to measure variations in the Bond work index values during the pre-treatment of the material to be crushed. A widely validated model that predicts the variation of the work index as a function of a process treatment does not exist yet. Nevertheless, experimental data exist [14] that could be useful for developing a new model for material pre-treatment. However, two major inconveniences appear: (i) this pre-treatment could have high energy requirements, even exceeding the original comminution process; and (ii) the work index value presents large uncertainties depending on the method used for its measurement and sample taking.

Some of the standard measurement procedures of Bond index values used in industry are listed here [5]:

- Bond Pendulum test.
- Narayanan and Whitens rebound pendulum test.
- JKMRC drop test.
- Bond ball mill grinding test.
- Bond rod mill grinding test.

b) **Approach B:** modifying machinery design parameters to redirect the power usage of the equipment (vibration-deformation) and surroundings (heat-noise) into material stresses, more likely to increase the utilization of energy into disrupting the internal structure of the material. Thus, promoting surface area creation due to rupture and abrasion.

This second approach is taken in the present thesis as means of modelling and further optimizing energy usage of comminution machinery. Particularly Paper I applies this approach to a jaw crusher.

It is common practice to define the efficiency of any kind of process as the ratio between the real behaviour an ideal behaviour of a system. Nevertheless, to establish the ideal comparison performance of a crushing and grinding machine, where seemly random breakage of particles occurs, represents no easy task. Consequently, there is not a standardized definition of comminution efficiency [5, 15, 6, 16, 17]. Definitions vary from being based on single particle breakage comparison in ball mills [6], to efficiency values based on crushed particle size distributions [17] and even in terms of thermal efficiency [18] as temperature increase in the crushing chamber of diverse devises.

In the current research the energy usage ($E_{Equipment}$) of the comminution process is defined as the measurement of the surface area (S) before and after crushing and grinding of the material, written as its derivative:

$$\frac{dE_{Equipment}}{dS} = kS^n \tag{2.1}$$

where k and n are constants related to the strength of the rock. The most widely numerical values used correspond to the Bond theory, with $n = -1.5$ and $k = W_i/2$, since they are relevant for most of the ranges of crushing and grinding processes in industry (Table 2.1) [19]. Other authors have defined different values for these constants, such as $n = -2$ and $k = C_R$ for Rittingers's theory, or $n = -1$ and $k = C_K$ for Kick's theory. These theories have different ranges of applicability, Kick's equation is applicable for large particle crushing (coarse crushing) and Rittinger's is used for describing the milling process of small particle size (ultra fine grinding). W_i is the average standard work index for crushing and grinding, defined by Bond [20], as the work input required to reduce ore from an infinite size to a size of 100 μm. Note that for repeated measurements with samples of the same material a wide range values could be found.

Table. 2.1 Terminology used in comminution and equation adequate coefficients use [19].

Size range of the product	Term used	Adequate coefficients
1 - 0.1 m	Coarse crushing	Kick
0.1 m	Crushing	Kick and Bond
1 cm	Fine crushing, coarse grinding	Bond
1 mm	Intermediate grinding, milling	Bond
100 μm	Fine grinding	Bond
10 μm	Ultra fine grinding	Rittinger

Therefore, for the present work an efficiency is defined in terms of the increase of specific surface energy $\Delta\ S_{EN}$ approximated by equation (2.2). Based on terms of the surface mean diameter of the particles before and after crushing. In order to estimate the crack propagation area increase per unit mass, as the ideal energy requirement of the process. As suggested by Tromans and Meech [3], with energy requierements based on mean size diameters; taking into account the effect of the size reduction process in a real machinery [17] and including the natural properties of the rock by means of the material fracture surface energy [21].

$$\Delta S_{EN} = \frac{\gamma A_{Created}}{M} \simeq \frac{6F_R\gamma}{\rho}\left(\frac{1}{D_{fsm}} + \frac{1}{D_{ism}}\right) \tag{2.2}$$

Thus ΔS_{EN} is expressed in SI units as $[J/kg]$, where $\gamma\ [J/m^2]$ represents the material fracture surface energy, $M\ [kg]$ is the total mass, $A_{Created}$ $[m^2]$ is the new surface area created, $\rho\ [kg/m^3]$ is the material density, $D_{ism}\ [m]$ is the initial surface mean diameter of the particles, $D_{fsm}\ [m]$ is the final surface mean diameter of the broken particles and F_R [dimensionless] $\in [1-3]$ is the surface roughness factor that takes into account that milled particles are not perfectly spherical.

The real energy usage is simply defined as the integral of the actual machine power usage over time. Taking as starting point the real energy consumption of $E_{Equipment}\ [J/kg]$, it is necessary to establish an energy

efficiency definition that takes into account the particle size reduction. Based on the classical definition of efficiency and aim for the increase in specific surface energy ΔS_{EN} $[J/kg]$ as the ideal energy requirement of the process, a classical efficiency of the equipment can be defined simply as the ratio between these two terms.

Since an efficiency on these terms results in values of the order $<1\%$ [21], it is necessary to normalize this value to increase its sensibility by the theoretical limit value of an ideal vertical crack propagating in a sphere η_{Limit} with values between 5% and 10% as function of the Possion's ratio of the material [3]. Thus, the total energy efficiency of the equipment is defined as:

$$\eta_{EnergyTotal} = \frac{\Delta S_{EN}}{E_{equipment}} / \eta_{Limit} \tag{2.3}$$

This versatile definition allows for an approximation of area created in terms of particle's diameter. Furthermore, it permits evaluating this ideal value both experimentally and numerically via sieve analysis or direct area increase obtained from simulations.

Correspondingly, the present research developments propose a single genetic optimization algorithm for comminution machinery in terms of semi-empirical design parameters. In terms of the previous energy use definition using semi-empirical models (for the case of jaw crushers), a set of equations is obtained based on energy not depending on the machinery design. To estimate the ideal performance of a comminution one can consider the increase in specific surface energy per unit mass. Thus, transforming the energy total efficiency into a power total efficiency:

$$\eta_{PowerTotal} = \frac{\Delta S_{Power}}{P_{equipment}} / \eta_{Limit} \tag{2.4}$$

A normalized mass flow of 1 kg/s is assumed, thus this value is not actually an impartial indicative of energy efficiency. However, it is useful

to evaluate how the power consumption of the machinery is influenced by its design parameters.

2.3 Jaw crushers

This thesis section is focused on experimental work, and model improvement on comminution machinery that aims at finding relations betwen both approaches. A jaw crusher is taken as a representative example. As one of the most important stages in industrial comminution is the initial size reduction process, where jaw crushers are most widely used. Their design basis is to impart an impact on a rock particle between a fixed and a moving plate [5] is advantageous during first stage crushing, where high magnitude forces are needed. A classical jaw crusher drawing is presented in (Fig.1).

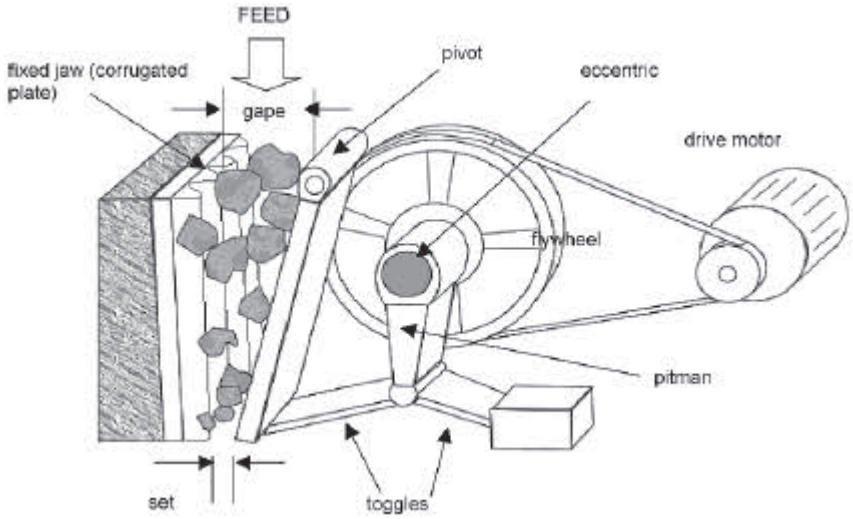

Fig. 1. Jaw crusher sketch [5].

2.4 Modelling of jaw crushers

For this thesis two main modelling areas for comminution equipment model are explored. First, an approach based on empirical models to further optimize a jaw crusher in terms of power usage through a simple genetic algorithm analysis. Second, a more descriptive method to model particle breakage using discrete element method (DEM) simulations.

2.4.1 Simple genetic algorithm analysis

Evolutionary algorithms are highly stochastic numerical methods that mimic the natural evolution/survival of a fitness function to locate its global optima [22]. Evolutionary algorithms are mainly associated with two of their most important types: a) Simple genetic algorithms (SGA) and b) Differential evolution methods.

The simple genetic algorithm methods (SGA) are aleatory search numerical schemes that locate the global (or local) maxima or minima of a function. This technique is based on different principles from the traditional deterministic methods based on interval bi-section and recurrent derivation such as Newton-Raphson, steepest descent, Bolzano's methods, among others. Since SGA methods have a lot of similitude with the natural evolution of species process, thus the same terms are used in both natural evolution and SGA optimization schemes [22].

The overall scheme of SGA methods is based on improvement of a random initial solution, called initial population by the evaluation of the individuals (using a fitness function), followed by reproduction of the population with a roulette wheel pair selection algorithm is made, with a probability of reproduction proportional to the better qualification of their solutions. Random mutations on the offspring are also introduced. Then, all the process repeats itself for several generations until a reliable solution is found. These are in principle the basic operators in a SGA method. Alternative function operators can be also implemented, such as reproduction of new solutions with more than

two parents, elitism, among others [23].

Differential evolution methods (DE) are evolutionary algorithms for a real coded genetic algorithm, this is one of the fastest converging and reasonably robust. In (DE) schemes it is not possible to define lower or upper limit boundaries, thus penalizing functions must be used to keep the search algorithm in a determinate area. The principal difference between DE and SGA algorithms is the operator differential mutation. For the current research, SGA algorithms are selected over DE methods, since, the latter ones presented (in practice), convergence difficulties finding solutions within their restrictive search area.

In the current research work the following operators where implemented on the SGA code that allowed to reach a solution for the jaw crusher optimization case:

- **Decimal form:** Defines the decimal form a binary string number.
- **Mapping:** Maps real decimal values into bit strings.
- **Evaluation:** Evaluates the function to optimize. This operator includes the handling of restriction functions.
- **Roulette wheel:** Parents of each generation are selecting using a roulette wheel selection algorithm proportional to how optimal is each solution on the parent selection pool.
- **Parent selection mechanism:** Defines the matrix containing the parents of a generation by random re-arranging.
- **Uniform cross over:** Alternative operator that performs cross over of the parents matrix by a flipping coin algorithm for each allele to produce the first child of the offspring. Then, an opposite copy of each gene is used to define the second child of this parent pair.
- **Mutation:** An aleatory mutation is introduced to the offspring of each generation. There is a restriction of maximum 2% of mutation probability.

- **Elitism:** Alternative fitness based selection operator. This operator forces the algorithm to retain at least one copy of the fittest solution found per generation.

As a multivariate optimization approach have been applied on crushers, in the area of flow sheet design [24]. In contrast, the application for the current study is centered on the power usage optimization due to variation in the parameter design of jaw crushers as machinery. This optimization is evaluated using a semi-empirical set of equations developed by Rose and English [25]. These set of equations and restriction functions are designed to describe reasonable well the real operation of jaw crusher. This model is mainly based on the charge capacity of the crusher chamber. Furthermore, it is also based on the time taken and distance travelled by the crushed rocks between the two opposite crusher plates, while these rocks being cyclically submitted to compression forces between the jaws [25].

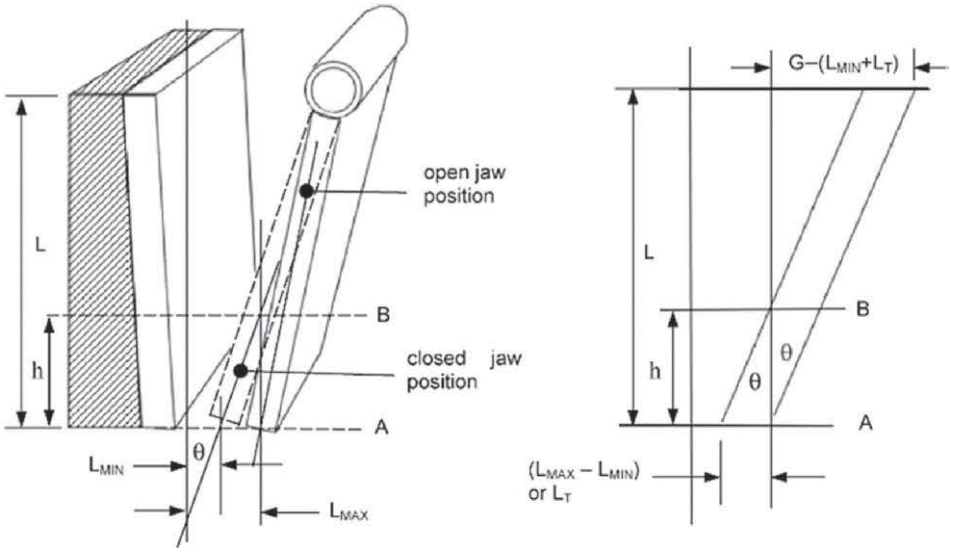

Fig. 2. Jaw crusher geometric parameters [25].

The geometric parameters or this model are presented in (Fig. 2) and the primary optimization variables are presented in (Table 2.2). It was concluded that a multi-variable search of the main machinery design

specifications (dimensions, rotational speed of the toggle, feeding flow and machine restrictions) affects the power consumption of the process, a global maximum of power efficiency is found when the reduction ratio of the crushing jaw is at its largest. Contour plots of the mutual influence of the machinery design variables can be observed in (Fig.3). Results were calculated with a precision of 50 digits in binary code for each variable and solution convergence was found at 500 generations.

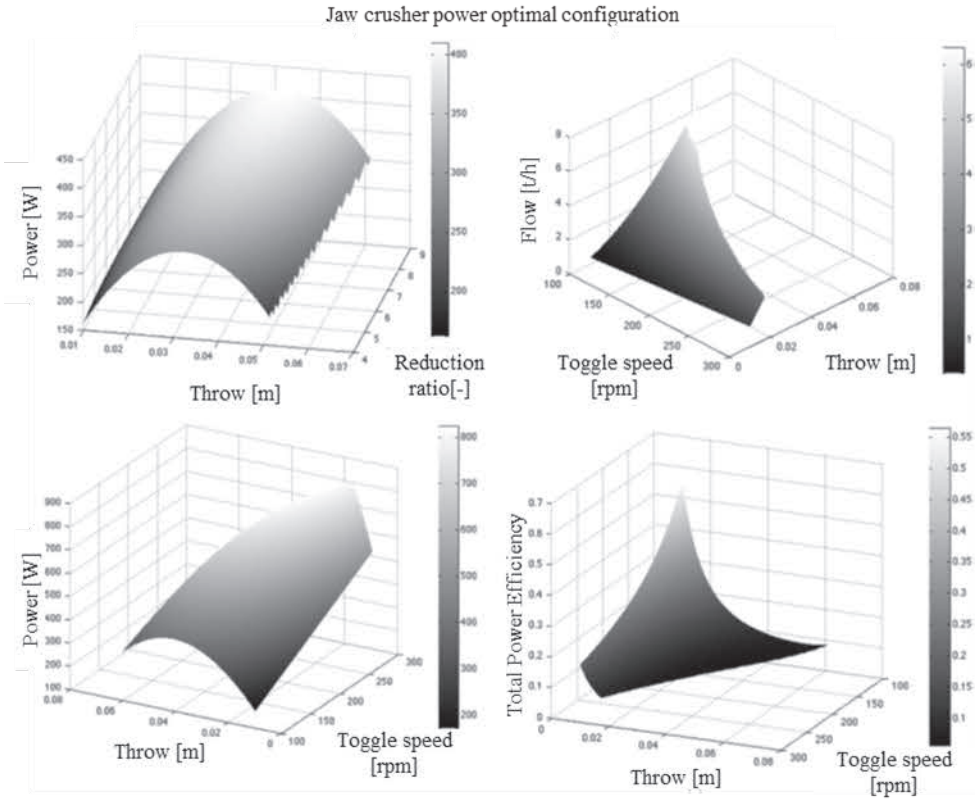

Fig. 3. Jaw crusher performance plots.

Table 2.2 Primary model variables and ranges (Paper I).

Variable	Symbol	Unit	Lower limit	Upper Limit
Gape	G	m	0.1	1.6
Reduction ratio	R	-	4	9
Toggle speed	Ω	rpm	100	300
Width	w	m	0.15	2.10
Throw	L_t	m	0.07	0.1
Min. passing % feed to the crusher	Min_{per}	%	1	80

A further reasoning on the selection of an optimization scheme based on SGA methods over traditional deterministic methods is based on the characteristics of the multivariable Rose and English [25] equation set. Even if multiobjective linear programming schemes, have the capacity to search for optimal values in a large search space, they are limited to sets of linearized equations. The Rose and English [25] equations present non-linear parts that if where linearized, would imply that certain characteristics that the model attempt to capture would be lost. Furthermore, in comparison with traditional deterministic methods for non-linear equations, such as those based on interval, bisection and recurrent derivation (Newton-Raphson, steepest descend, Bolzano's methods, among others), although they work well on non linear equations without a large number of local optima peaks, they are normally restricted to continuous search space areas. Due to the nature of the restriction equations for the jaw crusher optimization scheme, certain areas of the search space are restricted by machinery constrains. Therefore, presenting a non-continuity in the allowed search space of all variables. In conclusion the SGA method, demonstrated to handle successfully both non-linearity of the equation set in question and the discontinuities presented in the model search space.

After publication of Paper I, new research in terms of fundamental models for jaw crushers involving the so-called toggle jaw kinematics [26] have been developed recently. In theory, these new models should be able to predict more accurate descriptions of jaw crushers performance. Perhaps the application of an optimization approach similar to an evolutionary algorithm, if applicable, could result in improved machinery designs.

2.4.2 Discrete element modelling

The goal of this section is to describe the macro scale crushing process using the smallest scale representative physics of the breakage phenomena. In this sense, it is assumed that all ore stones are composed of agglomerates of smaller spherical particles (meta-particles) [27, 9]. The structural integrity of the agglomerate is based on connecting bonds between neighboring particles proportional in strength to their respective overlap. For this section the software EDEM 2.4 [28] was used. The genesis of an agglomerate can be appreciated in (Fig. 4). The main characteristic of this approach is that a meta-particle is treated as a solid structure. When this agglomerate comes in contact with a surface, another agglomerate or a boundary force, the structural stresses are propagated, both into the inside particles due to internal interactions between particles and into their constituent bonds. As a result of these, stress propagation will lead to deformation and eventually into breakage if a maximum predetermine value of normal (σ_{max}) or tangential shear (τ_{max}) stress is locally reached.

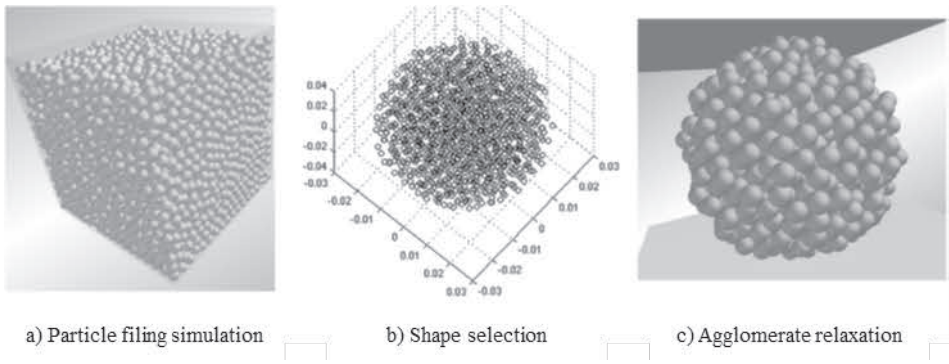

Fig. 4. Agglomerate genesis procedure.

Once an agglomerate is built, remains the task of calibrating its breakage behaviour. This is done through variations in particle sizes, bonds diameters and number, strength of the bond, or even in shape selection of the meta-particle. Schubert, Khanal and Tomas [29] provided a 2D DEM sphere model with direct impact on a flat surface at different velocities. Their calibration procedure was based on matching crack propagation patterns for concrete experimental rocks under similar

conditions as impact in rock simulations. Furthermore, their calibration procedure was accomplished with a combination of visual guidance and FEM analysis to observe the stress distribution on a spherical rock in similar laboratory conditions. Random particle size distribution was used in their agglomerate in contrast to a uniform micro-particle diameter used in the current research as means to simplify the model parameters of the simulation.

Another important calibration procedure was developed by Kempton et al. [30], where a successful particle simulation of the macro-deformation of a DEM cylindrical shape agglomerate under single compression by constant velocity moving plates. This simulation was successfully performed in a zero gravity environment. The current research calibration mechanism done in a gravity environment, in order to resemble (to some extent) the gravity effects of the crushed rock falling through the jaw crusher chamber.

Due to computational limitations, the variable to calibrate against the meta-particle is the material surface energy γ, in order to center computational efforts into variables directly related with energy usage. One benchmark research was developed by Herbst and Potapov [31], calibrating not only the material surface energy γ but also the Young modulus E, Poisson modulus ν through comparison with experimental single particle breakage by dropping weight mass experiments. It was shown that a material macroscopic behaviour can be reproduced when a large number of smaller particles are used per particle agglomerate, besides to the fact that small time steps are required for large number of small particles. Thus, this kind of calibration for several macroscopic variables can only be done with large computational resources.

Furthermore, a calibration procedure was proposed in terms of compression breakage of single agglomerate structures in a gravity environment (Fig.5). By modifications of the number and compaction of agglomerated particles, the simulated fracture surface energy ($\gamma_{Simulation}$) for a single particle calibration can be modified until resembles the actual fracture surface energy of a certain ore material. It was noticed that the agglomerate approaches the real material behaviour as the number of particles increases and the dimension of the bonds becomes smaller.

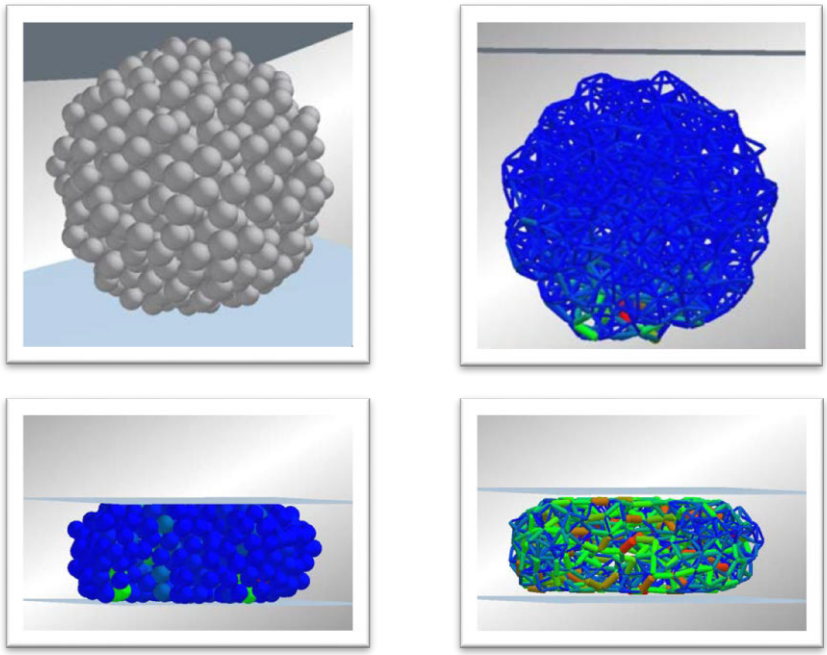

Fig. 5. Compression breakage of single agglomerate structures.

One of the principal parameters to define in a DEM soft particle simulation is the numerical time step. Within these kinds of models it is assumed that all the energy is transmitted via Rayleigh-waves. The Rayleigh time (T_R) is defined as the time propagation of a wave through a solid particle. This value can be approximated by [32]:

$$T_R = \pi R_{Particle} \sqrt{\left(\frac{\rho}{G_{Shear}}\right)} / (0.1631\nu + 0.8766) \tag{2.5}$$

Recommended simulation time step values oscillate between 0.1 T_R and 0.3 T_R [32]. These values should be carefully monitored since a large time integration step implies unrealistic large overlapp among particles. This leads to enormous force application over the simulated entities, producing acceleration peaks in the particles kinematics. The material modelled was magnetite, which has an elevated value of shear

modulus ($G_{Shear} = 28.17x10^9 Pa$), thus implying a small Rayleigh time, translating into larger computational requirements. Similar work by Refahi et al. [10] mentions a number superior to 4000 particles to perform a single particle breakage in a jaw crusher.

However, the calibration procedure had to be terminated on grounds of high computational time requirements and limited time available for the research, with a maximum number of bonds created of 9420 in a single agglomerate among 1249 particles. Instead, an attempt to model a jaw crusher was made using a particle agglomerate, which breakage pattern most resembled the actual breakage of a rock under compressing parallel plates. This simulation successfully demonstrated the capacities of DEM simulations to model the diverse stages of comminution in a jaw crusher (Fig.6).

These results are comparable to efforts made by Refahi et al. [10] for DEM jaw crusher simulations, although their research involved a larger number of particles per agglomerate ≅4000. Another important point is that their research was not only focused on spherical agglomerates, but also simulation of cubic agglomerate breakage by crack propagation comparison with experiments. Current DEM simulation research efforts are rather focused on energy usage, for which the simulation area increase for a particle breakage is defined in term of the number of broken bonds NBB within the agglomerate as:

$$A_{Created} = 2(NBB)\pi R_{Bond}^2 \tag{2.6}$$

Thus establishing a link with (Eq. 2.3) in terms of simulation parameters as:

$$\eta_{EnergyTotal} = \frac{\frac{\gamma_{simulation} A_{Created}}{M} / E_{Equipment}}{\eta_{Limit}} \tag{2.7}$$

Then, the influence of DEM simulations into estimations of equipment efficiency can be modelled. This implies that in principle DEM simulations can lead to improvements on energy usage in comminution machinery.

Current research trends show the power of similar DEM modelling on other crusher machinery at full-scale (particularly in cone crushers [33, 34]), demonstrating the capabilities of simulations, when the computational requirements are met.

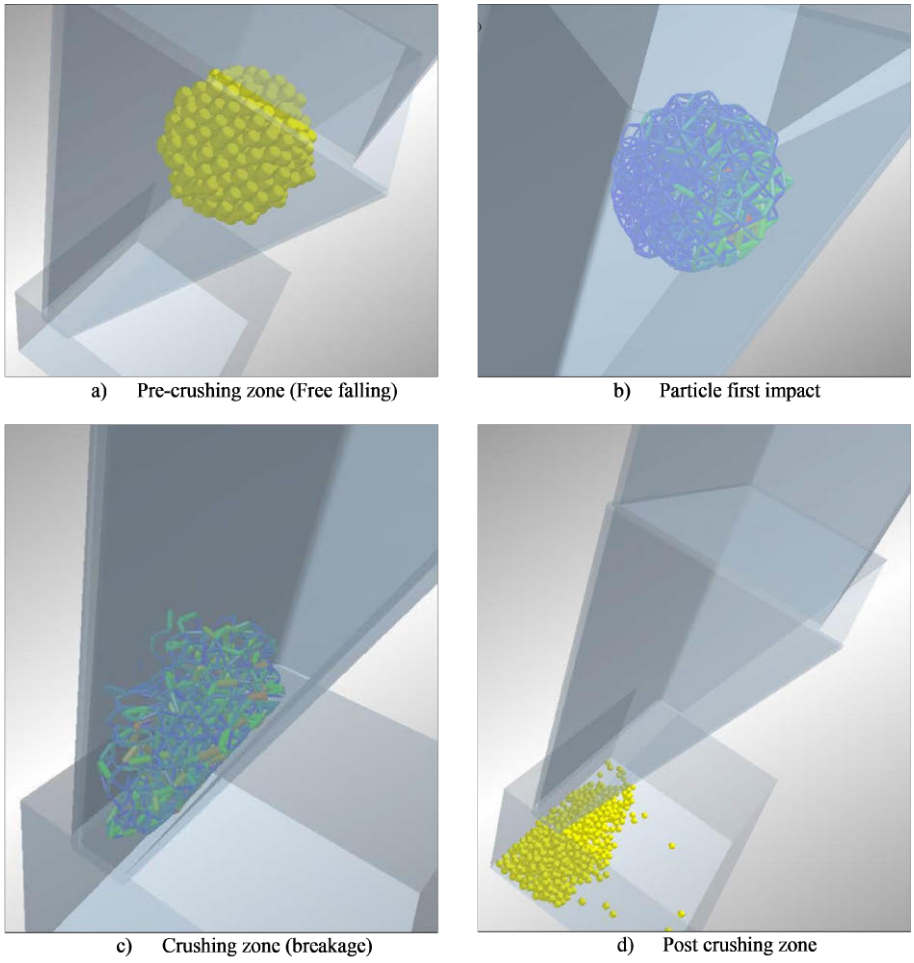

Fig. 6. Agglomerate breakage stages in a jaw crusher.

2.5 Experimental analysis

Finally, an experimental study was made using a Fristsch Jaw Crusher [35] available at Åbo Akademi laboratory for Geology and Mineralogy using limestone rock pieces of $\cong$ 600 gr (Fig.7) from Nordkalk's quarry at Parainen (Finland). These experiments are based on the measurement of area increment of the crushed rocks through sieve analysis. To investigate the operation mode of the crusher at different flow conditions, it was required to manipulate the jaw toggle velocity. The variable introduced was the rotational velocity of the jaw, for this purpose a frequency converter Optidrive 3GV [36] was used. Since decoupling the default mechanical belt transmission of the engine was inconvenient in terms of machinery replacement parts, such as construction of different transmission gears or conical belt holders. Therefore, it was preferable to manipulate the rotational speed of the motor using a variation in current frequency to affect the rotation of the electrical induction motor. The power consumption of the machinery was measured using PP264 60 A AC current clamps [37] and all data was recollected with a current Data Logger PicoLog CM3 USB/Ethernet [38].

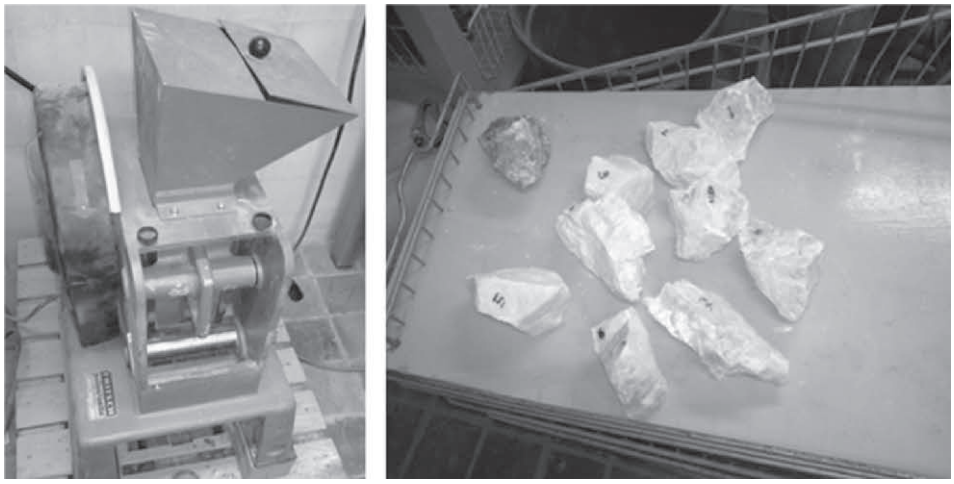

Fig. 7. Jaw crusher at ÅA Geology and Mineralogy laboratory and experiment rocks.

Experimental procedure per run

An experimental procedure is designed in order to estimate values of total energy efficiency (Eq.2.3), with the following steps:

- Measure the mass of the material (rock) to crush per each run.
- Start the jaw crusher.
- Vary the current frequency to the desired value.
- Wait until the system stabilizes.
- Introduce the material to crush carefully into the crusher feeding chamber.
- Measure the crushing time with a chronometer and record current consumption with the current clamps and the current data logger.
- Collect the crushed product in a storage bag and label it accordingly to the test set.
- Perform the sieve analysis and weigh the cumulative mass fraction on each sieve.
- Repeat for the next run at a different current frequency value.

Thus, with the recorded values, while the machinery is crushing, it was possible to calculate for every time instant the power consumption of the electrical tri-phase motor (P_{Elec}) driving the jaw crusher as [39]:

$$P_{Elec} = \sqrt{3} I_{rms} V_{rms} cos(\theta) \tag{2.8}$$

The actual comminution power consumption could be deduced from the difference of the power consumption of the functioning empty crusher and the recorded power consumption measured on the tri-phase electrical while rocks are being crushed:

$$P_{Comminution} = P_{Elec} - P_{Empty} \tag{2.9}$$

As the Bond work index (W_i) is related to the machinery shaft power consumption [20], an electrical efficiency of the motor must be taken into account, a value for $\eta_{Electric}$ of 80% was assumed. Then, the crusher power consumption at the crusher driving shaft is:

$$P_{Crusher} = \eta_{Electric} P_{Elec} \tag{2.10}$$

The average power consumption of the equipment is taken as the temporal average of the measured values:

$$P_{Equipment} = \frac{\int P_{Elec} dt}{\int dt} \tag{2.11}$$

Then, energy used to crush a certain amount of material at each run can be defined, using the material rock flow rough the machinery (Q_A):

$$E_{Equipment} = \frac{P_{Equipment}}{Q_A} \tag{2.12}$$

Crushed materials were processed via sieve analysis. Results showed no significant variations on the final mass fraction cumulative distribution curve as function of the jaw toggle rotational speed (Fig.8). Furthermore, values of total energy efficiency (Eq. 2.3) $\leq$ 6 % were found with mild variations around 1-2% among samples presumably due to shape deviations and different internal initial cracks on the ore.

Peak increments in the power consumption of the jaw crusher were found during experimental tests. With at least 30% increment in the power consumption while a limestone rock is crushed between the jaws of the equipment.

The experimental procedure proved to be easily reproducible. Furthermore, since it is based on area increment measurement, it can be ap-

plied on every size range of the crushed product, from coarse crushing (particle size 1-0.1 m) to ultra-fine grinding (particle size 10 μm).

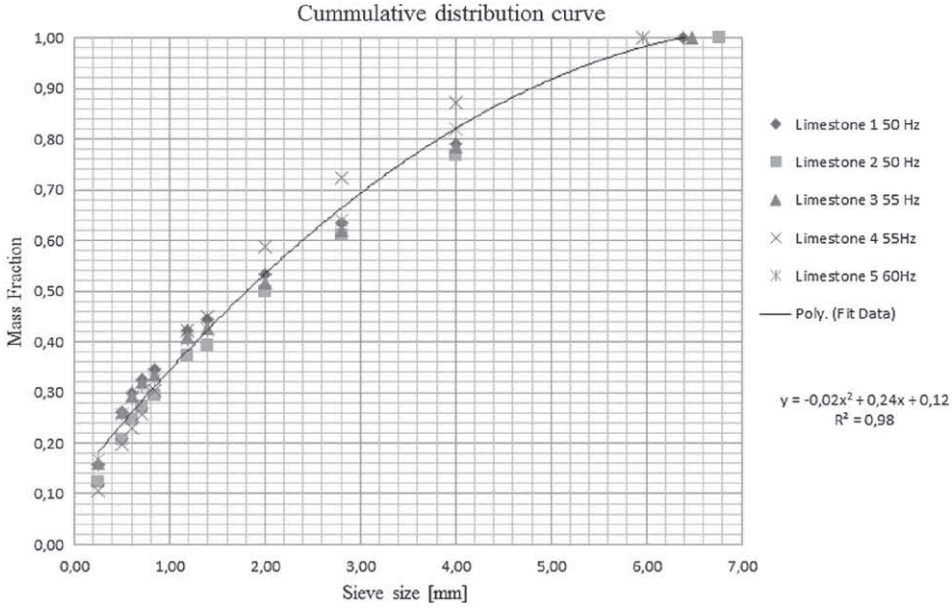

Fig. 8. Cumulative distribution curve.

Chapter 3

Bubble swarm dissolution

Mass transfer and chemical reactions in a bubble reactor represent an engineering design challenge even in today's world since it involves a complex mixture of a dispersed gas phase in an aqueous solution. Further experimenting, modelling and validation is still needed to be able to implement and develop models suitable for engineering processes design. Although is estimated that 25% of all reactions in chemical industry takes place in multiphase liquid-gas flows [40], bubble reactor engineering, despite modern attempts in initial modelling in bubble ozone dissolution [41], CFD simulations based on single bubble size models [42] or phase dispersed drag models [43]; numerical bubble dissolution methods are still closer to an art than a science because low-accuracy algorithms may disrupt the physics reflected by the models implemented [44]. One of such liquid-gas flows belong to the Slag2PCC process, more concisely on the bubble CO_2 capture reactor (Fig.9), in which dissolved calcium results in calcium carbonate precipitation (PCC) representing one of the efforts in the field of carbonation capture and storage [1, 2].

Therefore, to establish a concise model for bubble reactor design, the analysis of this physical system is essentially defined by the basic mass transfer phenomena for a single isolated bubble. After this, one may further extend the analysis to a scatter bubble swarm, and gradually increase the complexity of this swarm, i.e. increase of the local gas

fraction until an industrial scale operation process is reached. A previous CO_2 dissolution and conversion reactor at laboratory scale with a reactor height of 60 cm was found to be insufficiently tall for total bubble dissolution [2]. Therefore, the efforts of this research are focused on finding the optimal vessel height for complete dissolution of CO_2 bubbles in water. A column diameter of 127 mm is chosen as the first parameter design, due to space limitation and simplification of costs for laboratory purposes, scaling it to other slag2PCC set-ups at ÅA and Aalto university.

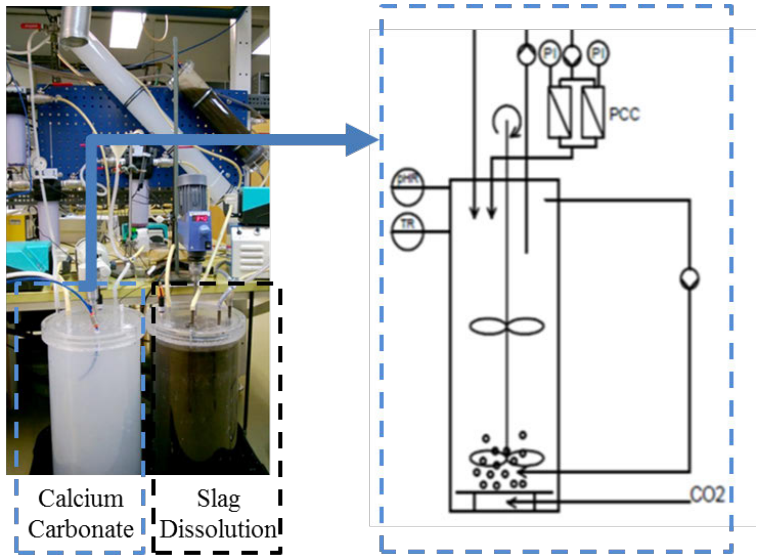

Fig. 9. Slag2PCC experimental set up (left) and calcium carbonate bubble reactor graphical representation (right) [2].

3.1 Historical overview

The relevant region for most common industrial applications of bubble columns is Re $= \mathcal{O}(10^3)$ according to Joshi [45]. This matches ranges of current numerical and experimental results of Re=1200-1500.

In terms of multiphase flow simulations, there have been several modelling attempts depending on the description of the bubble-fluid inter-

action phenomena. From single rising bubbles for moderate Reynolds numbers by Amaya-Bower and Lee [46] using the lattice Boltzmann method, where the shape evolution of the rising bubble can be modelled; to so-called sono-chemical reactors by Jamshidi and Brenner [47], where sound is the main cause for bubble diameter change. The model type closest to modelling efforts presented in this thesis, would be mass transfer of ozone dissolution in a bubble plume, by Gong et al. [41], where ozone bubbles reduce their size as they rise in coalescent fluid described using a two way coupling method.

The mass transfer model by Gong et al. [41], result in a simulation similar to the numerical efforts of bubble dissolution phenomena in the present thesis. Numerical methods present in the current research compendium aim at stirred environment flows which are characteristic of chemical reactors. Thus, the research questions for Paper II are established:

- Is it possible to perform a CFD simulation on CO_2 bubble dissolution in a stirred media?
- Is it possible to reach a 100% CO_2 dissolution in a scale suitable for the slag2PCC process within realistic reactor heights?

Experimental methods in bubbly flows are normally performed with the use of a camera set up as a non intrusive measurement device. This gives means to experimental assessment bubble shape, size, speed and dissolution rate [48]. Commonly rectangular towers are preferred over cilindrical ones to avoid optical distortion effects due the curvature of the reactor tank wall [49]. As it is known that single rising bubbles move upwards in spiral rising path [50], an image analysis algorithm such as the one presented in Paper III is needed to isolate a single rising entity and extract all its relevant information.

In the current research a first experimental approach was centred on a single raising and dissolving CO_2 bubble (Paper III). As every numerical method needs validation of its results, a third research question arises:

- What is needed to verify numerical simulation results on bubble CO_2 dissolution?

Further complexity of the on experimental set up facilities allow the extension from single bubble tracking to bubble swarm tracking. In literature, studies on bubble size distribution evolution along a bubble column exist, such as developed by Ferreira et al. [51], where a successful bubble size distribution of a swarm allowed for distinguishing three different classes of bubbles overlapping by their image analysis complexity level: (i) large complexity (several overlapping bubbles, bubbles might not be recognizable from each other); (ii) medium complexity bubbles (some overlapping present among entities, although bubbles can be easily distinguish from each other) and (iii) low complexity, i.e. single bubbles. Present experimental efforts are focused on lower gas area fractions $\leq 7\%$, thus allowing all recorded bubbles across the pipe to be treated as single bubbles. Moreover, errors derived from bubble (visual) overlapping should in principle be suppressed by statistical means given that a large bubble sample is used, particularly high-speed camera recording at 1000 frames per second as done in the current work.

An important study on bubbles size distributions by image analysis on a Plexiglas pipe with diameter 0.24 m and height 5 m, with a six arm sparger with holes as a bubble swarm source, puts emphasis on the evolution of the bubble swarm size distribution as means to understand the underlying dispersion physics of the system along the pipe height [52]. That study involved the air-water combination system in an impeller free environment. In contrast, the next step of the experimental analysis presented here aimed at a more realistic operating condition for bubble reactors, with bubble size distribution affected by the dissolution of CO_2 in water and a continuous impeller mixing effect that is hypothesized to increase dissolution rate as function of stirring intensity.

Thus, arises the following research question from Paper IV, as a first qualitative estimation:

- For operating conditions, as close to real applications for the

Slag2PCC process, how does the rotational speed of the mixing impeller affect the dissolution of the bubble column reactor?

With a more cautious quantitative analysis as the next step of the current research, numerical tracking methods and size analysis were improved to allow analysis of bubble swarms. Then, logically the following research questions appear in Paper V:

- Is a quantitative analysis based on bubble size distribution changes sufficient to explain the bubble dissolution phenomena in a bubble column reactor?
- What parameters are necessary to take into account in order to give a reliable description of the CO_2 bubble dissolution process?

3.2 Modelling

The first step to model a full bubble reactor is to focus on the analysis into its smallest yet representative mass transfer unit for a design process, i.e. a single dissolving bubble. It is important to analyze how the bubble movement (in a Newtonian fluid) is driven by buoyancy effects, fluid local velocity, pressure or shear patterns, fluid properties and complex fluid forces [53]. It is a common task in engineering design to model a bubble as spherical immersed body under the effect of different forces. Either punctual drag, lift, history forces acting on its center of mass or forces acting on its surface [53, 54]; as commonly modelled in industrial applications [55].

A set of expressions connecting the mass transfer boundary layer theory [56] and forces on a bubble through the mass time change rate [57] on a dissolving bubble, included as function of the local Reynolds, Schmidt [58] and Sherwood [59] numbers is established in terms of dimentional analysis [60]. With bubble drag [61], lift forces [62] and velocities disturbances due to bubble non-sphericity [63] can be calculated using empirical models, and further validated with experimental data related to mass transfer from single carbon dioxide bubbles in

contaminated water [64]. Basically, a combination on Newtons second law of motion and mass transfer through boundary layers can be established as seen in (Fig.10). This is the basis for the numerical bubble dissolution process.

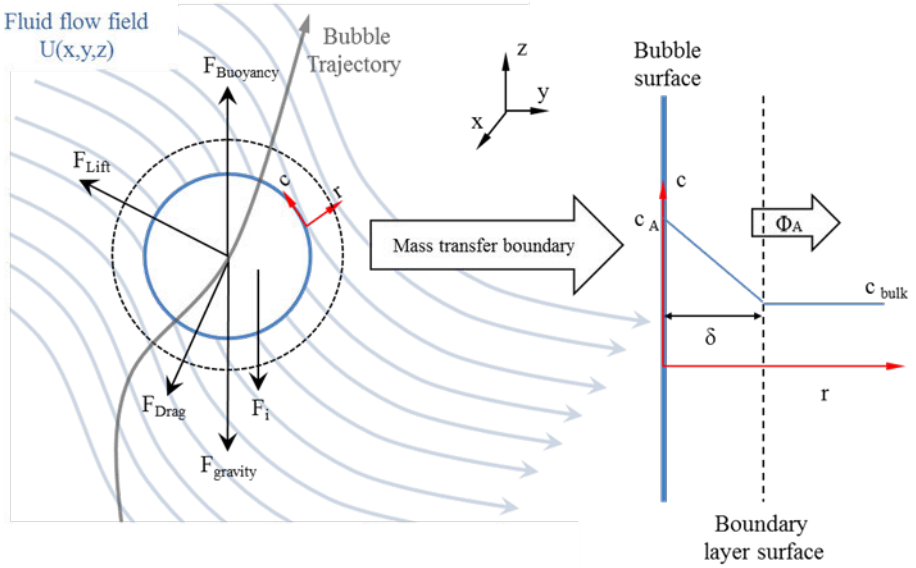

Fig. 10. Free body diagram with forces and mass transfer boundary [Paper II].

From this the following force balance equation is deducted:

$$\frac{d(m\overrightarrow{V}_{Bubble})}{dt} = \overrightarrow{F}_{Bouyancy} + \overrightarrow{F}_{gravity} + \overrightarrow{F}_{Drag} + \overrightarrow{F}_{Lift} + \sum \overrightarrow{F}_{i} \quad (3.1)$$

where F_i forces include fluid history effects, deformation effects, virtual mass force term and other bubble-fluid interaction forces. These forces are of essential for modelling bubbly flows. For the present numerical work several of these forces could be neglected in a first calculation to study the pure effect of the dissolution process. Later on with experimental verification, depending on deviations from experimental data, these forces may also be added.

The link with mass dissolution via bubble mass time ($\frac{dm}{dt}$) derivative is done using mass transfer theory [56]:

$$\frac{dm}{dt} = \phi_A = -k_{mass} A_{sup} (C_A - C_{Bulk}) \tag{3.2}$$

where the system mass transfer driving force depends on concentration difference between the bulk concentration of the surrounded liquid (C_{bulk}), the wet interface concentration of the bubble (C_A), mass transfer coefficient (k_{mass}) and bubble surface (A_{Sup}).

3.2.1 1D model

The one-dimensional model set up is a vertical projection of the previous model (Eq. 3.1). Therefore, the rising entities do only possess one degree of freedom while rising plus its consequence diameter reduction due to mass transfer. Even if a straight-line rising bubble does not describe the movement of a bubble rising in a stagnant aqueous solution. This estimation represents a fair starting point to assess the orders of magnitude of the dissolution process. This model implies the integration of a second order differential equation that to be solved required a variable step size integration routine. For this case, a Runge-Kutta Felhber method is used to define this variable step size as the difference between the fifth- and fourth-order error estimates [65]. Rough results from this model suggested a dissolution of a 5 mm CO_2 bubble in water at a vertical height of 1.6 m. Thus, giving a starting value of reactor height orders of magnitude.

3.2.2 One-way coupling disperse swarm dissolution

A one-way coupling model represents the next stage towards a realistic bubble column description. Not only the rising bubble movement in a 3 dimensional environment is included but also how its movement is

affected by the local velocity and pressure gradients of the surrounding fluid. Also, a stirred medium is added with a frozen rotor simulation, dividing the column in four sections each containing a pitched blade impeller scaled to the reactor diameter [66]. This simulation is performed using COMSOL Multiphysics v.5.2 software. Due to computational limitations the intercommunication of the different parts of the model was done in a simple one-way coupling fashion, thus the movement of the bubbles does not affect the fluid flow and other neighbor entities. These large simplifications can only be claimed valid for very dilute bubbly flows with low gas volume fractions and low interaction between particle induce turbulence and fluid flow turbulence [67]. Particularly for the present study a low gas fraction (0.008%) is present and the bubble induced kinetic energy in the fluid is negligible in comparison with the turbulent kinetic energy induce by the impeller mixing motion at 100 rpm. Hence, this model is applied to simulate the dissolution of a small swarm of 32 bubbles in a stirred column reactor (Fig.11). This produced very raw results on how to design an experimental facility to further improve the capabilities of the model.

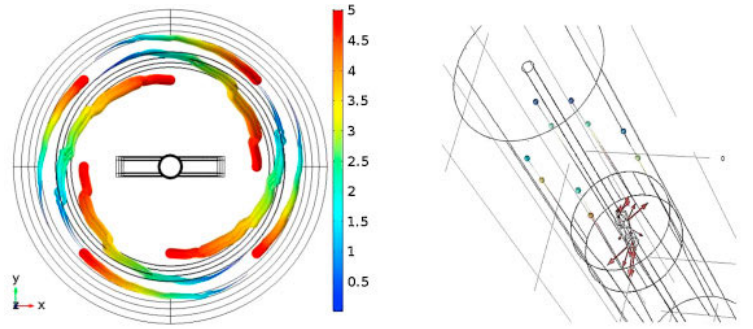

Fig. 11. Bubble undulating trajectories in a bubble tower.

The one way coupling model allowed to predict a complete bubble swarm (initial size 5 mm) dissolution at a height of 1.95 m after 8.5 s (Fig.11). With these predictions the construction of a reactor of similar dimensions was started. Results are comparable to a two-way coupling application of dissolving ozone bubble plumes in a rectangular tank of 40 cm height by Gong et al [41]. Moreover, another similarity is found

when comparing the non-linear dependency of bubble diameter with the dissolution rate of ozone for the case of Gong et al. [41] and CO_2 for the present case. A large difference is, however, found in terms of applications since in the current research work, the numerical efforts were centred on finding the reactor height for total CO_2 bubble dissolution (1.95 m) rather than to study the distribution of dissolved gas in the liquid phase [41].

3.3 Experimental analysis

Using as starting point, the raw estimations of the disperse swarm model (Section 3.2.2), a bubble of initial D_{Bubble}= 5 mm, at low volume fraction results on complete dissolution height of 1.95 m. Therefore, a system with similar height specifications was built using a Plexiglas transparent pipe of diameter, D= 127 mm and height, H=2 m, as seen in (Fig.12) and a pH meter is used to verify at each time low CO_2 concentration in the liquid phase of the system. In a separate experiment using a pH colour indicator, it was verified that vertical pH variations in the column are very quickly balanced. Bubbles are feed into the system through a perforated flange (perforated diameter=0.5 mm), and gas flow (air or CO_2) controlled using a needle valve.

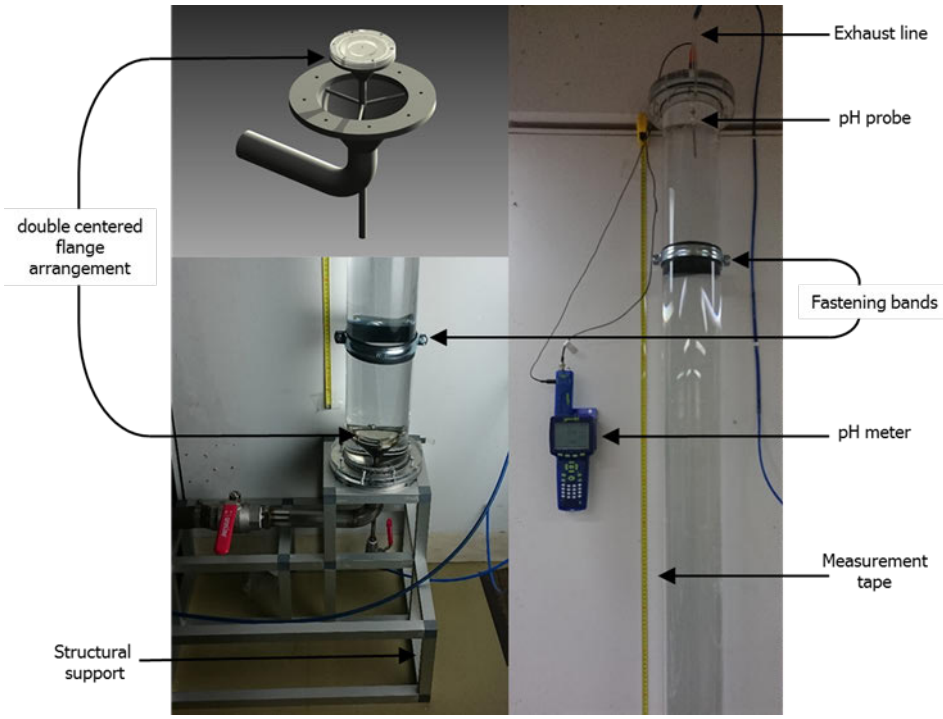

Fig. 12. Experimental set up.

3.3.1 A single dissolving bubble

The first experimental approach is centered on the rising-dissolution phenomena of a single rising bubble, using a high-speed Photrom camera SA3 Model 120K-M3 equipped with a 52 mm Nikon 200733 lense and a distance of 1-1.5 m to visualize a window of 45 cm and 20 cm of the bubble tower at different heights, as seen in (Fig.13). The spatial resolution of the system is 2.4 – 4.45 pixel/mm at a rate of 1000 images per second with a constant exposure of 1/2000.

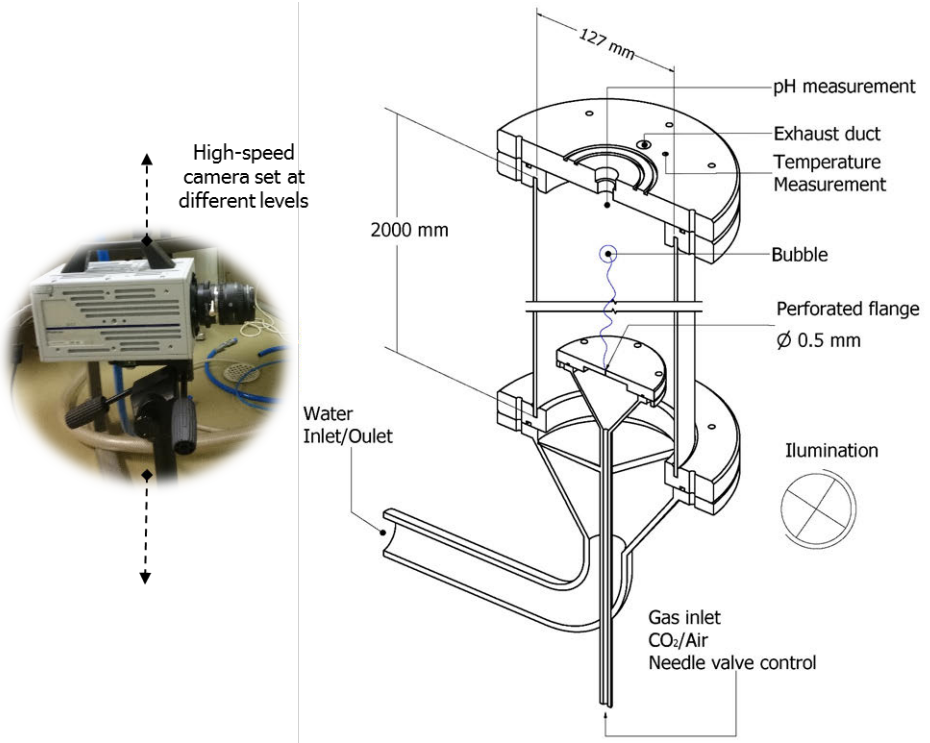

Fig. 13. Cross section of the bubble column and high-speed camera placement

An image analysis algorithm was developed using Matlab image processing toolbox. Several authors previously had used a similar technique for single CO_2 bubbles ≤ 3 mm in a rectngular tank until a maximun vertical possition of 60 cm [68] and the study of oxigen mass transfer of dense bubble swarms at high volume fraction ($\leq 16,5\%$)

[69] and further higher volume fractions ($\leq 30\%$) using signals froma an optical probe [70]. For this first experimental procedure the technique is based on:

- Removal of the background.
- Threshold iteration for B&W conversion.
- Size position filtering.
- Edge detection and filing of structures.
- Size, shape and position estimation in base of a reference point.
- Ellipse fit.

An example of this procedure can be appreciated in (Fig.14). All bubbles are approximated by a surrounding oblate spheroid with a major semi-axis b and a minor semi-axis a, which are measured from the two dimensional constrains from an ellipse fit. Thus, an equivalent spherical bubble diameter can be defined (Eq. 3.3). These approximations are common in the image analysis of free rising bubbles. One important example is given by Colombet et al. [70], with research applied to image analysis of dense bubble swarms, enabling to determine experimentally the overall mass transfer phenomena of a very dense group of free rising bubbles.

$$D_{Bubble} = \left(8b^2a\right)^{\frac{1}{3}} \tag{3.3}$$

Furthermore, to estimate the bubble rising shape evolution along the bubble column a secondary variable is defined as the bubble aspect ratio χ of these ellipses:

$$\chi = \frac{b}{a} \tag{3.4}$$

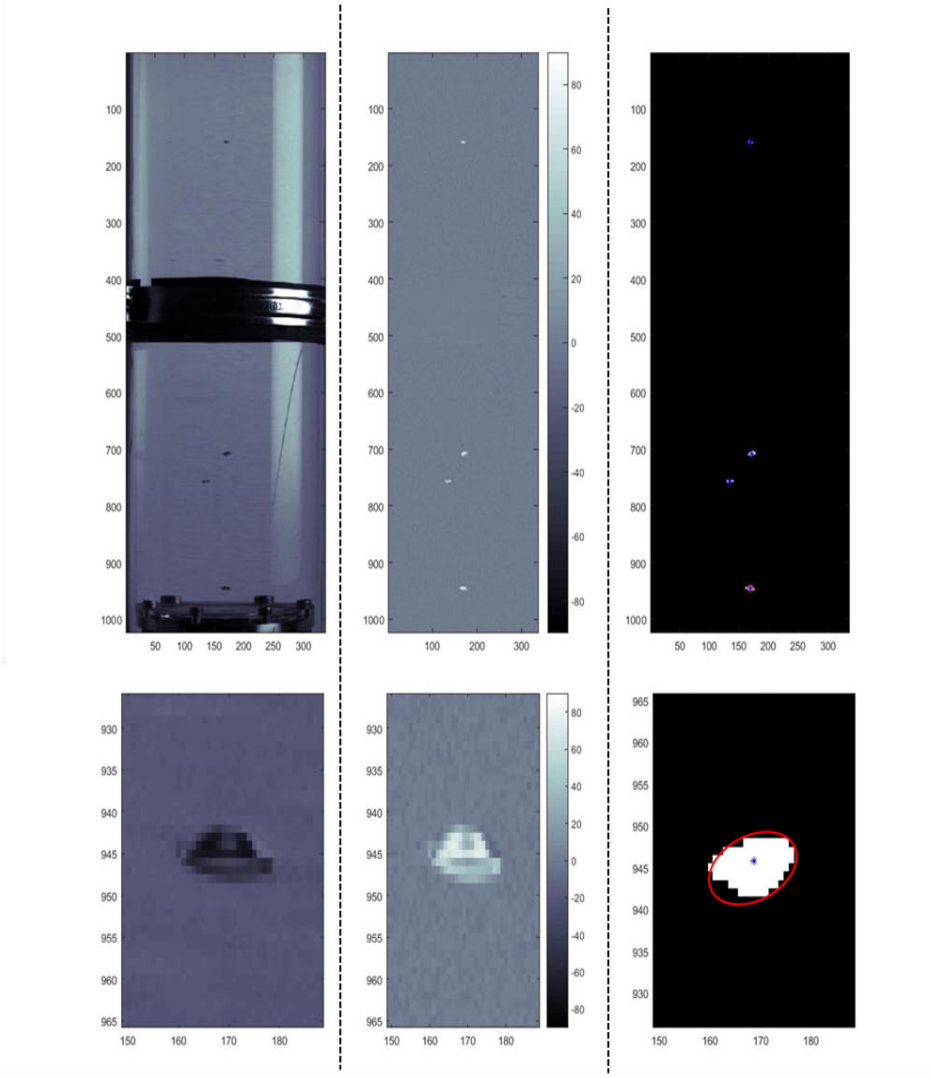

Fig. 14. Image processing.

Besides CO_2, a second set of experiments was performed using air as a control set. Results showed dissolution of a single CO_2 rising bubble of diameter approximately 5 mm with close resemblance to the models previously proposed (Fig. 15 b) for the 2 m high bubble column. The camera was not able to detect the smallest bubbles at the last (highest) stages of the experimental set up.

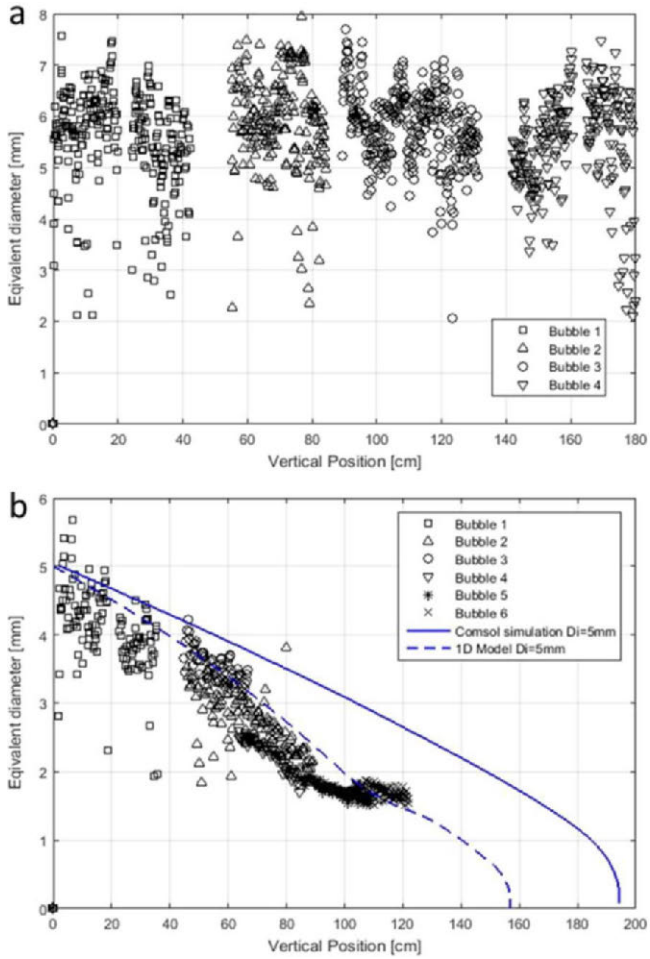

Fig. 15. Bubble dissolution, diameter reduction. (a) Air, (b) CO_2.

Furthermore, for air no clear correlation in terms of bubble diameter with vertical position of the bubble tower can be appreciated in (Fig.15 a). As expected the air flow used as a control experiment shows no clear signs of dissolution for the measured heights.

However, one of the most important findings of this experiment is the shape transition of the dissolving bubbles. Initially a wobbling undulating behaviour can be observed towards an ellipsoidal transition shape to finally spherical shape bubbles with linear rising trajectories (Fig.16).

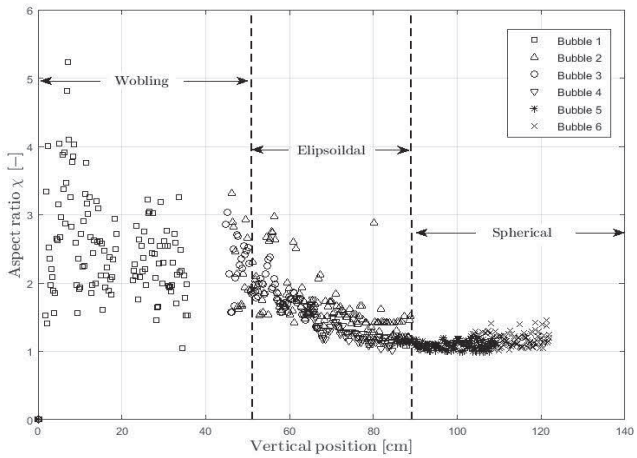

Fig. 16. Bubble aspect ratio vs. vertical bubble position.

3.3.2 Bubble swarm dissolution

Finally, the inclusion of impellers in the system is used to resemble the actual stirring environment of an industrial reactor (Fig.17). Bubble swarms of 58-140 bubbles are tracked using a similar camera set up as in the previous section. This time the image frames of study are around the center (horizontal) line of the four impellers inside the bubble tower. Given in Paper IV is a qualitative estimation of the CO_2 bubble dissolution at different impeller rotational speeds, showing higher dissolution rates at higher speeds. However, the nature of the dissolution swarm cannot be fully explained in terms of simple visual analysis. Paper V proposes a quantitative image analysis measurement technique for this new system. The spatial resolution of the system is 6.9 pixel/mm at a rate of 1000 images per second with a constant exposure of 1/2000. A control set of experiments with air bubbles is also conduced, with bubbles not showing signs of dissolution.

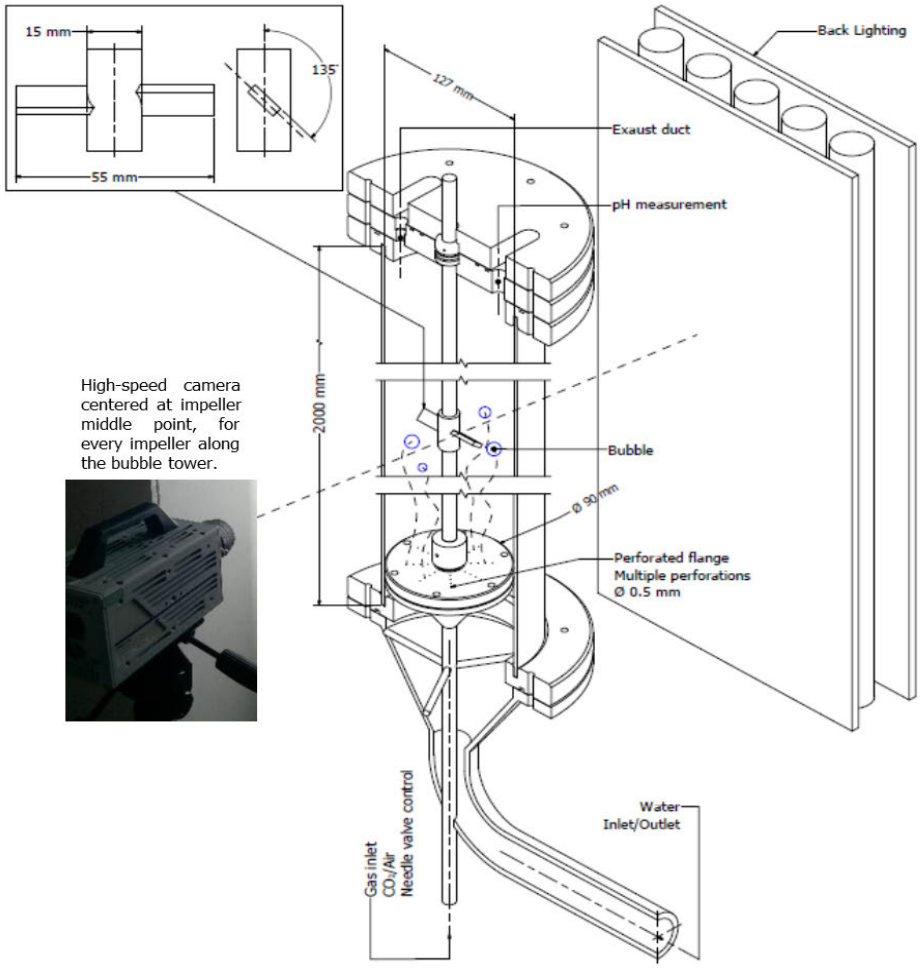

Fig. 17. Semi-cross section of the bubble reactor with high-speed camera placement and back lighting.

The image analysis of bubble swarm dissolution in a stirred reactor implies a higher complexity that a single bubble tracking algorithm. A significant number of bubbles overlap periodically as they rise, while distortion effects due the reactor wall curvature become noteworthy. Moreover, impeller motion obstructs the field of view of the camera, and also multiple bubble lock on tracking becomes more computationally demanding. An improvement of the single bubble tracking algo-

rithm was made based on:

- Background synchronization.
- Optics distortion correction.
- Filtering and contrast enhancement.
- Level set for B&W conversion.
- Size and shape estimation.

Previous studies on the free rising behavior of bubble swarms in water using statistical methods [71] had managed to produce reliable results of the dynamics of bubbles. In contrast, in addition to the inclusion of impellers, this investigation attempted to give a reliable description of the bubble swarm dissolution. With the study of different heights of a bubble reactor through a measurement of bubble size distributions in each of the four reactor sections. Results show an evolution of the CO_2 size distribution towards smaller diameters as function of height. Moreover, a clear reduction of the Sauter mean diameter from initially 3.52 mm to 1.50 mm at the fourth and highest reactor section was observed (Fig.18).

It is important to notice that bubbles in a complex fluid flow configuration with impellers present a spiral path rising behaviour. Especially for wobbly shape rising bubbles the approximation of axi-symmetry might not be completely accurate. Fujiwara et al. [50] performed similar experiments on a bubble column with the use of a second shadowgraphy camera and succeeded producing a 3D bubble swarm reconstruction by means of image integration. Moreover, other miss-accuracy errors might arise since in highly rotational flow conditions such as a mixing reactor. Errors such as overlapping bubbles, bubbles oscillating in and out from the plain of focus, bubbles passing behind the impeller or the impeller shaft, among others. These errors in principle could be minimized with the use of a second recording camera in a perpendicular plane respect to the first original camera. Unfortunately a second camera wasn't available and it could not be purchased or rented within reasonable expenses for the project. Nonetheless, the use

of a second shadowsgraphy camera (and the background lights/lamps equipment for it) is recommended for future research in similar systems.

Through comparison of the current swarm CO_2 dissolution measurements at 100 rpm (Fig.19), a fair match was obtained for the experimental swarm bubble Sauter diameter to the estimations and experiments of single bubble rising, at least for the first three (lowest) column sections. In the highest section the dissolution rate seems to decrease and the diameter approaches results of the one-way model simulation presented above. Which can be explained by the very low volume fraction of dispersed bubbles in this section.

In terms of the effect of the rotational speed on the dissolution process, it was concluded that a small diameter reduction of 20-10% occurs as a result of changing the impeller speed from 0-100 rpm and from 100 to 200 rpm on equivalent reactor heights. Even if the Sauter mean diameter of a CO_2 bubble swarm seems to follow, up to a certain extent, the dissolution behavior of a single free rising bubble; the dissolution dynamics of the swarm cannot be explained by just one parameter (similar to previous work done using empirical correlation parameter fitting, such as using a unique longitudinal dispersion coefficient [72]). Therefore, a study on the size distributions through a Weibull distribution fit [73] is proposed.

Even if a qualitative analysis of the images in the right side of (Fig. 18) can lead to the conclusion that bubbles seem to dissolve, this does not provide enough information to compare the bubble size distribution evolution on the impeller locations. The quantitative analysis presented in the left side of (Fig. 18) allows to compare how the Sauter mean diameter shift towards smaller bubble sizes. Not only does bubble mean size decrease, but also the distribution is largely compressed towards smaller bubble sizes.

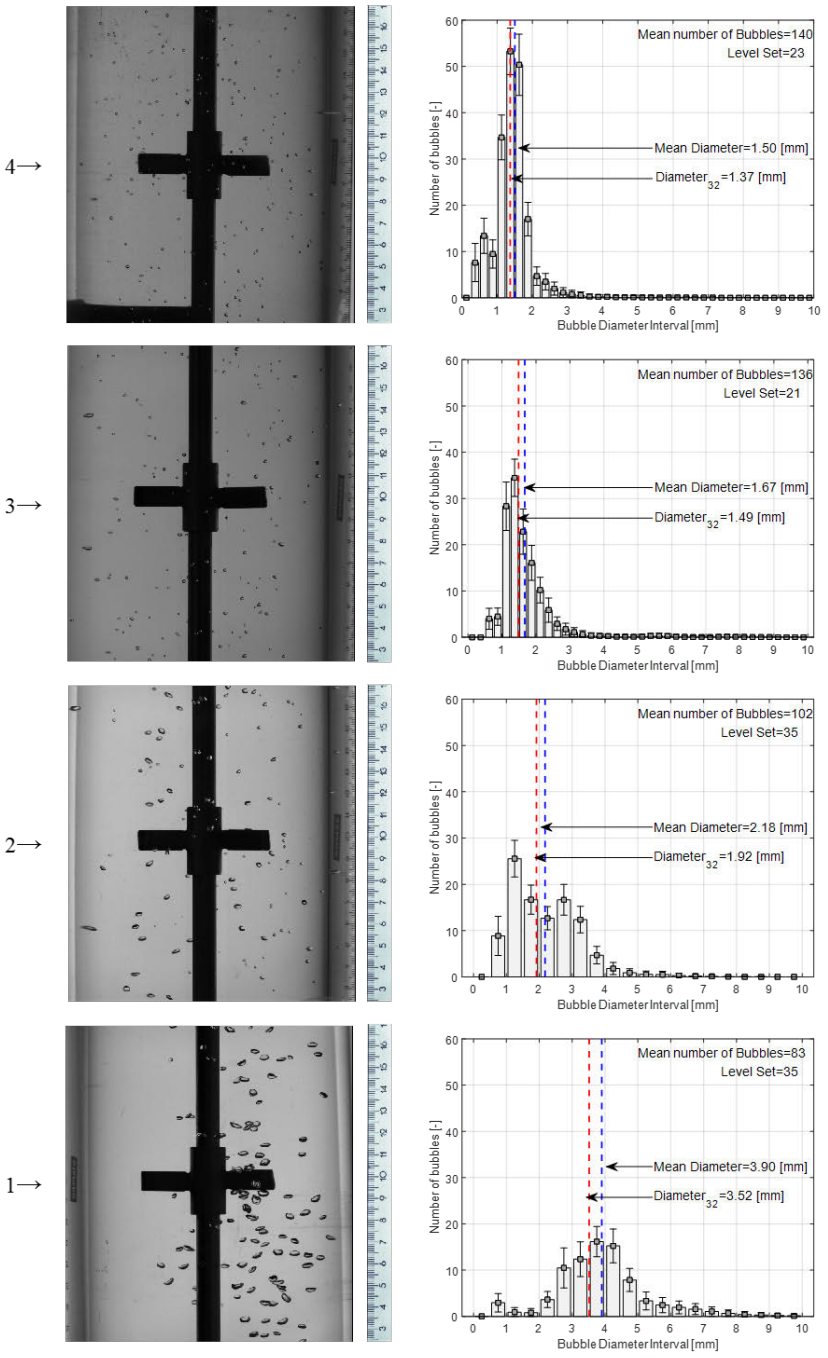

Fig. 18. CO_2 dissolution, impeller N^o and bubble size distribution.

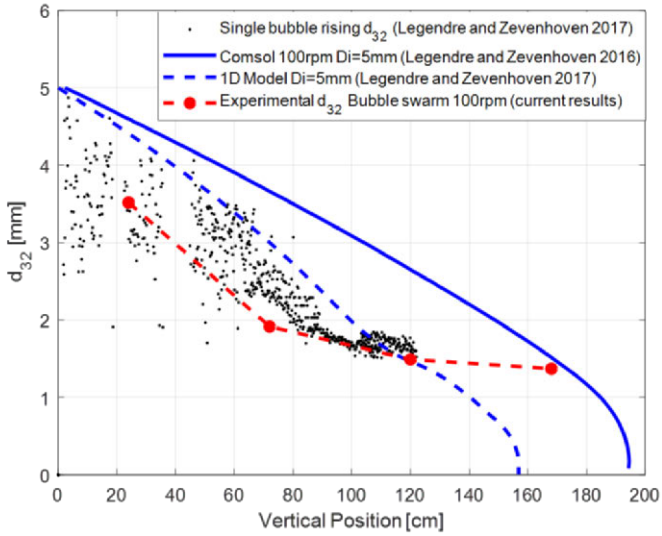

Fig. 19. Bubble CO_2 dissolution, Sauter diameter reduction.

To give an accurate comparison of the bubble size distributions at different impeller locations, the distributions were normalized to a probability density function (pdf) for all diameter intervals. The Weibull distribution is selected for its versatility to adapt to reducing size data such as survival analysis data [74] and the present case. The Weibull pdf depends on two parameters that influence its behaviour, the shape parameter c and the scale parameter d. The Weibull pdf for a variable x is defined as:

$$\mathcal{F}_{Weilbull}(x|c,d) = \frac{d}{c}\left(\frac{x}{c}\right)^{d-1} e^{-(x/c)^d} \tag{3.5}$$

Results allow us to conclude that a study of bubble swarm dissolution in terms of only bubble mean diameters is insufficient. However, the inclusion of their bubble probability density distribution shape represents a more suitable description on bubble swarm dissolution nature. As it can be appreciated in (Fig.20), the bubble pdf presents a clear change not only in size, but also in frequency of smaller elements as the bubble rise. Thus, these results can lead to improve simulation efforts in cases such as a two- or even a four-way coupling simulations.

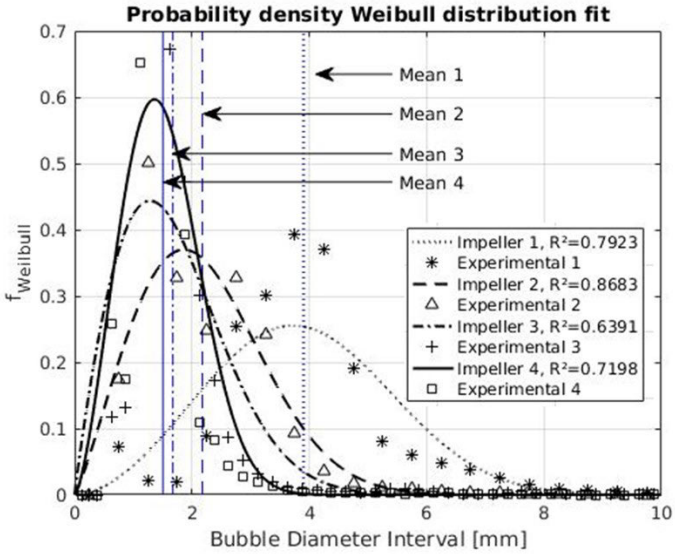

Fig. 20. Probability density distribution fit, CO_2 dissolution.

Chapter 4

Conclusions and future work

This thesis is focused on the numerical and experimental analysis of two types of process equipment: bubble swarm dissolution in a bubble column and comminution of ore materials in a jaw crusher. Even though numerical efforts are very different, the underlying state of the art of modelling such devices is comparable. The modelling efforts are based on a clear definition of the smallest relevant physical phenomena of the systems studied. For the crushing and grinding case this is the breakage of agglomerates modelled as the bond rupture between two spherical particles. On the other side for the bubble dissolution case it is needed to establish a link between single bubble dynamics and its surrounding mass transfer boundary layer.

For both systems experimental procedures were designed, developed and tested with the aim to compare and improve numerical simulations. In a jaw crusher a total energy efficiency value was measured as function of crushed rock sieve analysis. Nevertheless, this method is in principle applicable to all kinds of comminution equipment regardless of its size or type. A first stage DEM simulation for a jaw crusher was programmed, demonstrating its enormous potential in this field, with the downside of high computational requirements. After that work was done and reported, new research has been published by others, demonstrating the capacities of a DEM simulation using computer clusters. Future simulations on jaw crushers could be used to evaluate

machinery performance in terms of jaw surface design. For example, a curved or corrugated jaw could be more beneficial for impact crushing than a flat jaw. Furthermore, this can be extended to optimization and development of other types of crushers, mills and grinders. Additionally, FEM stress analysis on crack propagation could complement DEM agglomerate breakage simulations.

In terms of bubble swarm dissolution, a model that estimates bubble size reduction due to dissolution was established and published. Results were comparable to experimental analysis of single rising bubbles and of that Sauter mean diameter for bubble swarms. Nevertheless, it was concluded that to fully explain the bubble swarm dissolution of a reactor; the discussion must be established in terms of bubble probability density distributions and their shape evolution. Still is to be culminated a two-way coupling model for bubble reactors, for which a computer cluster is necessary, while commercial CFD codes do not readily support two-way coupling simulations with the desired conditions for this work. Such a model would allow to reach higher gas volume fractions, closer to actual reactor operating conditions.

Perhaps a LES simulation for the agitated fluid could be useful to define smaller flow fluctuations that would allow a more accurate interaction with the dissolving bubbles. A four-way coupling might be not feasible to compute for the present reactor operating conditions, due to quite large computational requirements. Finally, future comparisons with the results measured for bubble swarms using a high-speed camera could aid improvement of CFD models for higher gas volume fractions.

Bibliography

[1] A. Said, T. Laukkanen, and M. Järvinen, "Pilot-scale experimental work on carbon dioxide sequestration using steelmaking slag," *Applied Energy*, vol. 177, pp. 602–611, 2016. [Online]. Available: http://dx.doi.org/10.1016/j.apenergy.2016.05.136

[2] H.-P. Mattila and R. Zevenhoven, "Design of a continuous process setup for precipitated calcium carbonate production from steel converter slag." *ChemSusChem.*, vol. 3, pp. 903–913, 2014.

[3] D. Tromans and J. Meech, "Mineral comminution: Energy efficiency considerations," *Minerals Engineering*, vol. 21, pp. 603–620, 2008.

[4] K. Holmberg, P. Kivikytö-Reponen, P. Härkisaari, K. Valtonen, and A. Erdemir, "Global energy consumption due to friction and wear in the mining industry," *Tribology International*, vol. 115, pp. 116–139, 2017.

[5] A. Gupta and D. Yan, *Mineral Processing design and Operations an Introduction*. Amsterdam, The Netherlands: Elsevier, 2006.

[6] D. W. Fuerstenau and A. Z. Abouzeid, "The energy efficiency of ball milling in comminution," *International Journal of Mineral Processing*, vol. 67, pp. 161–185, 2002.

[7] K. Schoenert, "On the limitation of energy saving in milling," in *1. World Congress Particle Technology, Part II, Comminution, Nurnberg, April 16–19*, 1986, pp. 16–19.

[8] S. Mortsell and J. Svensson, "Discussion of a paper entitled: a new surface measurement tool for mineral engineers, by F.W. Bloecher, Jr." in *Trans. AIME, 190, pp. 981-983*, 1951.

[9] D. O. Potyondy and P. A. Cundall, "A bonded-particle model for rock," *International Journal of Rock Mechanics and Mining Sciences*, vol. 41, pp. 1329–1364, 2004.

[10] A. Refahi, J. A. Mohandesi, and B. Rezai, "Comparison between bond crushing energy and fracture energy of rocks in a jaw crusher using numerical simulation," *Journal of the Southern African Institute of Mining and Metallurgy*, vol. 109, pp. 709–717, 2009.

[11] D. Legendre, "Assesing the energy eficiency of jaw crushers," M.Sc. Thesis, Åbo Akademi University: Turku, Finland, 2012.

[12] J. Richardson and J. Harker, *Chemical engineering-Volume 2: Particle Technology and Separation Processes*, 5th ed. Oxford, England: Elsevier Ltd, 2002.

[13] D. Tromans and J. Meech, "Fracture toughness and surface energies of minerals: estimates for oxides, sulphides, silicates and halides," *Minerals Engineering*, vol. 15, pp. 1027–1041, 2002.

[14] J. Ruskanen, "Influence of Rock Properties on Compressive Crusher Performance," PhD Thesis, Doctoral dissertation. Tampere University of Technology, 2006.

[15] N. Djordjevic, "Improvement of energy efficiency of rock comminution through reduction of thermal losses," *Minerals Engineering*, vol. 23, pp. 1237–1244, 2010.

[16] L. M. Tavares, "Optimum routes for particle breakage by impact," *Powder Technology*, vol. 142, pp. 81–91, 2004.

[17] W. Carey and C. Stairman, "A method of assessing the grinding efficiency of industrial equipment," *Recent Developments in Mineral Dressing. London*, pp. 117–133, 1953.

[18] A. Schelinger, "A calorimetric method for studying grinding in a tumbling medium," *Trans. AIME*, vol. 190, pp. 518–522, 1951.

[19] M. Rhodes, *Introduction to particle technology*. England: John Wiley and Sons, 1998.

[20] F. C. Bond, "Crushing and grinding calculations," *Allis Chalmers Publication*, no. 07R9235B, pp. 1–14, 1961.

[21] D. Tromans and J. A. Meech, "Fracture toughness and surface energies of covalent minerals: Theoretical estimates," *Minerals Engineering*, vol. 17, no. 1, pp. 1–15, 2004.

[22] F. Pettersson, *Evolutionary algoritms. Course material 424511*. Turku, Finland: Åbo Akademi University, 2012.

[23] K. Miettinen, P. Neittaanmäki, M. Mäkelä, and J. Periaux, *Recent advances in genetic algorithms, evolution strategies, evolutionary programming, genetic programming and industrial applications*. Baffins Lane, Chicheste, West Sussex PO19 1UD, England: John Wiley & Sons, LTD., 1990.

[24] L. While, L. Barone, P. Hingston, S. Huband, D. Tuppurainen, and R. Bearman, "A multi-objective evolutionary algorithm approach for crusher optimisation and flowsheet design," *Minerals Engineering*, vol. 17, no. 11-12, pp. 1063–1074, 2004.

[25] A. Gupta and D. Yan, *Mineral processing design and operations an introduction*. Amsterdam, The Netherlands: Elsevier, 2006.

[26] M. Johansson, M. Bengtsson, M. Evertsson, and E. Hulthén, "A fundamental model of an industrial-scale jaw crusher," *Minerals Engineering*, vol. 105, pp. 69–78, 2017.

[27] H. Masamuda, H. K, and H. Yoshida, *Powder Technology Handbook.*, 3rd ed. Boca Raton (FL): Taylor and Francis Group, 2006.

[28] DEM Solutions Ltd (2009)., "DEM Solutions, Ltd." 2011. [Online]. Available: http://www.dem-solutions.com

[29] W. Schubert, M. Khanal, and J. Tomas, "Impact crushing of particle-particle compounds - Experiment and simulation," *International Journal of Mineral Processing*, vol. 75, no. 1-2, pp. 41–52, 2005.

[30] L. Kempton, D. Pinson, S. Chew, P. Zulli, and A. Yu, "Simulation of macroscopic deformation using a sub-particle DEM approach," *Powder Technology*, vol. 223, pp. 19–26, 2012.

[31] J. A. Herbst and A. V. Potapov, "Making a discrete grain breakage model practical for comminution equipment performance simulation," *Powder Technology*, vol. 143-144, pp. 144–150, 2004.

[32] K. Christoph, *Liggghts, Granular Materials. Open source DEM*. Austria: Material course, 2011.

[33] P. W. Cleary, M. D. Sinnott, R. D. Morrison, S. Cummins, and G. W. Delaney, "Analysis of cone crusher performance with changes in material properties and operating conditions using DEM," *Minerals Engineering*, vol. 100, pp. 49–70, 2017.

[34] J. Quist and C. M. Evertsson, "Cone crusher modelling and simulation using DEM," *Minerals Engineering*, vol. 85, pp. 92–105, 2016.

[35] Fritsch, "Jaw crusher "Pulverisette1". Operating manual," 2012. [Online]. Available: http://www.fritsch-milling.com

[36] Invertek, "Optidrive 3GV user's guide," 2012. [Online]. Available: http://www.invertek.co.uk/product{_}optirive{_}plus3vip.aspx

[37] Picotech, "Current clamp PP264. User's guide." 2012. [Online]. Available: http://accessories.picotech.com/current-clamps.html

[38] ——, "User's guide. Current data loger CM3," 2012. [Online]. Available: http://www.picotech.com/current-data-logger.html

[39] S. J. Chapman, *Maquinas Electricas*, third edit ed. McGraw-Hill, 2000.

[40] M. Martín, M. Galán, R. Cerro, and F. Montes, "Shape oscillating bubbles: hydrodynamics and mass transfer - a review," *Bubble Science, Engineering & Technology*, vol. 3, no. 2, pp. 48–63, 2011.

[41] X. Gong, S. Takagi, H. Huang, and Y. Matsumoto, "A numerical study of mass transfer of ozone dissolution in bubble plumes with an Euler – Lagrange method," *Chemical Engineering Science*, vol. 62, pp. 1081–1093, 2007.

[42] Z. Huang, D. D. McClure, G. W. Barton, D. F. Fletcher, and J. M. Kavanagh, "Assessment of the impact of bubble size modelling in CFD simulations of alternative bubble column configurations operating in the heterogeneous regime," *Chemical*

Engineering Science, vol. 186, pp. 88–101, 2018. [Online]. Available: https://doi.org/10.1016/j.ces.2018.04.025

[43] S. Wang, K. Zhang, S. Xu, and X. Yang, "Assessment of a bubble-based bi-disperse drag model for the simulation of a bubbling fluidized bed with a binary mixture," *Powder Technology*, vol. 338, pp. 280–288, 2018. [Online]. Available: https://linkinghub.elsevier.com/retrieve/pii/S0032591018304716

[44] H. A. Jakobsen, "Phase distribution phenomena in two-phase bubble column reactors," *Chemical Engineering Science*, vol. 56, pp. 1049–1056, 2001.

[45] J. B. Joshi, "Computational flow modelling and design of bubble column reactors," *Chemical Engineering Science*, vol. 56, pp. 5893–5933, 2001.

[46] L. Amaya-bower and T. Lee, "Computers & Fluids Single bubble rising dynamics for moderate Reynolds number using Lattice Boltzmann Method," *Computers and Fluids*, vol. 39, no. 7, pp. 1191–1207, 2010. [Online]. Available: http://dx.doi.org/10.1016/j.compfluid.2010.03.003

[47] R. Jamshidi and G. Brenner, "An Euler-Lagrange method considering bubble radial dynamics for modeling sonochemical reactors," *Ultrasonics Sonochemistry*, vol. 21, no. 1, pp. 154–161, 2014.

[48] M. Maldonado, J. J. Quinn, C. O. Gomez, and J. A. Finch, "An experimental study examining the relationship between bubble shape and rise velocity," *Chemical Engineering Science*, vol. 98, pp. 7–11, 2013. [Online]. Available: http://dx.doi.org/10.1016/j.ces.2013.04.050

[49] L. Böhm, T. Kurita, K. Kimura, and M. Kraume, "Rising behaviour of single bubbles in narrow rectangular channels in Newtonian and non-Newtonian liquids," *International Journal of Multiphase Flow*, vol. 65, pp. 11–23, 2014. [Online]. Available: http://dx.doi.org/10.1016/j.ijmultiphaseflow.2014.05.001

[50] A. Fujiwara, Y. Danmoto, K. Hishida, and M. Maeda, "Bubble deformation and flow structure measured by double shadow images and PIV / LIF," *Experiments in Fluids*, vol. 36, pp. 157–165, 2004.

[51] A. Ferreira, G. Pereira, J. A. Teixeira, and F. Rocha, "Statistical tool combined with image analysis to characterize hydrodynamics and mass transfer in a bubble column," *Chemical Engineering Journal*, vol. 180, pp. 216–228, 2012. [Online]. Available: http://dx.doi.org/10.1016/j.cej.2011.09.117

[52] G. Besagni, P. Brazzale, A. Fiocca, and F. Inzoli, "Estimation of bubble size distributions and shapes in two-phase bubble column using image analysis and optical probes," *Flow Measurement and Instrumentation*, vol. 52, pp. 190–207, 2016. [Online]. Available: http://dx.doi.org/10.1016/j.flowmeasinst.2016.10.008

[53] E. Michaelides, *Particles, Bubbles & Drops: Thier Motion, Heat and Mass Transfer.* Singapore: World Scientific Publishing Co. Pvt. Ltd, 2006.

[54] A. A. Kulkarni, "Lift force on bubbles in a bubble column reactor: Experimental analysis," *Chemical Engineering Science*, vol. 63, no. 6, pp. 1710–1723, 2008.

[55] J. B. Joshi, "Computational flow modelling and design of bubble column reactors," *Chemical Engineering Science*, vol. 56, no. 21-22, pp. 5893–5933, 2001.

[56] W. McCabe, S. J., and P. Harriot, *Unit Operations of Chemical Engineering*. New York: McGraw-Hill, 1993.

[57] W. Beek, K. Mutzall, and J. Van Heuven, *Transport Phenomena*. USA.: Wiley, 1999.

[58] F. Takemura and A. Yabe, "Gas dissolution process of spherical rising gas bubbles," *Chemical Engineering Science*, vol. 53, no. 15, pp. 2691–2699, 1998.

[59] A. Chernoutsan, A. Polyaniin, A. Manzhirov, V. Polyaniin, V. Popov, B. Putyatin, Y. Repina, V. Safrai, and A. Zhurov, *A consice Handbook of Mathematics, Physics and Engineering Sciences.* USA.: CRC Press Taylor & Francis group, 2011.

[60] K. Hanjalic, S. Kenjeres, and H. Jonker, *Analysis and Modelling of Physical Transport Phenomena.* The Netherlands: VSSD, Delf., 2007.

[61] I. Roghair, Y. M. Lau, N. G. Deen, H. M. Slagter, M. W. Baltussen, M. Van Sint Annaland, and J. A. Kuipers, "On the drag force of bubbles in bubble swarms at intermediate and high Reynolds numbers," *Chemical Engineering Science*, vol. 66, no. 14, pp. 3204–3211, 2011.

[62] T. R. Auton, "The lift force on a spherical rotational flow," *J . Fluid Mech*, vol. 183, pp. 199–218, 1987.

[63] W. Dijkhuizen, I. Roghair, M. V. S. Annaland, and J. A. M. Kuipers, "DNS of gas bubbles behaviour using an improved 3D front tracking model-Model development," *Chemical Engineering Science*, vol. 65, no. 4, pp. 1427–1437, 2010.

[64] J. Aoki, K. Hayashi, and A. Tomiyama, "Mass transfer from single carbon dioxide bubbles in contaminated water in a vertical pipe," *International Journal of Heat and Mass Transfer*, vol. 83, pp. 652–658, 2015. [Online]. Available: http://dx.doi.org/10.1016/j.ijheatmasstransfer.2014.12.062

[65] S. C. Chapra and R. P. Canale, *Numerical Methods for Engineers*, sixth edit ed. New York: McGraw-Hill, 2010.

[66] N. P. Cheremisinoff, *Handbook of Chemical Processing Equipment*, E. group, Ed. United States of America: Butterworth-Heinemann, 2000.

[67] T. Strömgen, "Model predictions of turbulent gas-particle shear flows," Ph.D. Thesis, Doctoral dissertation. KTH, University. Stockholm Sweden., 2010.

[68] W. J. Nock, S. Heaven, and C. J. Banks, "Mass transfer and gas – liquid interface properties of single CO2 bubbles rising in tap water," *Chemical Engineering Science*, vol. 140, pp. 171–178, 2016. [Online]. Available: http://dx.doi.org/10.1016/j.ces.2015.10.001

[69] D. Colombet, D. Legendre, A. Cockx, P. Guiraud, F. Risso, C. Daniel, and S. Galinat, "Experimental study of mass transfer in a dense bubble swarm," *Chemical Engineering Science*, vol. 66, no. 14, pp. 3432–3440, 2011. [Online]. Available: http://dx.doi.org/10.1016/j.ces.2011.01.020

[70] D. Colombet, D. Legendre, F. Risso, A. Cockx, and P. Guiraud, "Dynamics and mass transfer of rising bubbles in a homogenous swarm at large gas volume fraction," *Journal of fluid Mechanics*, vol. 763, pp. 254–285, 2014.

[71] G. Besagni and F. Inzoli, "Comprehensive experimental investigation of counter-current bubble column hydrodynamics: Holdup, flow regime transition, bubble size distributions and local flow properties," *Chemical Engineering Science*, vol. 146, pp. 259–290, 2016. [Online]. Available: http://dx.doi.org/10.1016/j.ces.2016.02.043

[72] Y. Ohki and H. Inoue, "Longitudinal mixing of the liquid phase in bubble columns," *Chemical Engineering Science*, vol. 25, no. 1, pp. 1–16, 1970.

[73] S. Kotz, N. Balakrishnan, and N. L. Johnson, *Continuos Multivariate Distributions. Volume 1: Models and Applications.*, second edi ed. Canada: John Wiley & Sons, Inc., 2000.

[74] H. E. Pham, *Springer Handbook of Engineering Stadistics*. NJ 08854, USA: Springer-Verlag London Limited, 2006.

ISBN 978-952-12-3822-2
ISBN 978-952-12-3823-9 (pdf)
Painosalama Oy
Turku, Finland 2019